Received: 26 June 2021 | Revised: 1 August 2021 | Accepted: 18 August 2021

DOI: 10.1002/inf2.12270

REVIEW ARTICLE

WILEY

Morphology control in high-efficiency all-polymer solar cells

Kangkang Zhou[1] | **Kaihu Xian**[1] | **Long Ye**[1,2]

[1]School of Materials Science and Engineering, Tianjin Key Laboratory of Molecular Optoelectronic Sciences, Tianjin University, Tianjin, China

[2]State Key Laboratory of Applied Optics, Changchun Institute of Optics, Fine Mechanics and Physics, Chinese Academy of Sciences, Changchun, China

Correspondence
Long Ye, School of Materials Science and Engineering, Tianjin Key Laboratory of Molecular Optoelectronic Sciences, Tianjin University, Tianjin, China.
Email: yelong@tju.edu.cn

Funding information
National Natural Science Foundation of China, Grant/Award Number: 52073207; State Key Laboratory of Applied Optics, Grant/Award Number: SKLAO2021001A17; Peiyang Scholar program from Tianjin University

Abstract

All-polymer solar cells (All-PSCs) have attracted tremendous research interest in the recent decade due to the great potentials in stretchable electronic applications in terms of long-term stability and mechanical stretchability. Driven by the molecular design of novel polymer acceptors and morphology optimization, the power conversion efficiency (PCE) of All-PSCs has developed rapidly and now exceeded 17%. This review outlines the promising strategies for high-performance All-PSCs from the aspect of morphology control with the motivation to rationally guide the optimization. In this review, we briefly discuss the thermodynamic mixing principles of all-polymer blends and the effects of the molecular structure of conjugated polymers on thin-film morphology in All-PSCs. The crucial role of molecular miscibility in influencing morphological features and performance metrics was highlighted. We also expound on the effective methods of controlling film morphology through properly tuning the aggregation behavior of polymers. In particular, insightful studies on the commonly used naphthalene diimide-based acceptor polymers and the newly emerging polymerized nonfullerene small molecule acceptors (ITIC-series, Y6 -series, etc) are discussed in detail. Finally, we present an outlook on the major challenges and the new opportunities of All-PSCs for efficiency breakthroughs targeting 20%.

KEYWORDS

aggregated structure, all-polymer solar cells, morphology tuning, photovoltaic polymers, polymer acceptor

1 | INTRODUCTION

With the exhaustion of fossil energy such as oil, coal, and natural gas, there is an urgent need for humans to find new substitutes to meet the development of our society. In the past three decades, photovoltaic energy has developed rapidly and has been recognized as a promising way to deal with future energy crises.[1] In particular, polymer solar cells (PSCs) are receiving increasing attention for their great potential for eco-friendly roll-to-roll processing. In addition, lightweight, high transparency, and high stretchability are the promising features of PSCs.[2–5]

Solar cells based on polymer donor: polymer acceptor blends,[6–8] also called all-polymer solar cells (All-PSCs), have exhibited great potentials in stretchable electronic applications in terms of morphological stability and mechanical stretchability.[9–11] Before 2014, the progress of All-PSCs was very sluggish, which was mainly limited by

the inferior electron transport performance of polymer acceptors and the undesirable morphology and very few choices of polymer donors: polymer acceptors blends.[12] Afterwards, naphthalene diimide (NDI)[13] and perylene diimide (PDI)[14]-based polymers with high electron mobility were widely used as polymer acceptors to improve the powered conversion efficiency (PCE) of All-PSCs. Recently, a breakthrough has been made in high-efficiency All-PSCs by polymerizing small molecule acceptors, being actively created and modified in the PSC community. For example, by employing a Y6-based polymer acceptor, Min et al.[15] obtained the PCE of 17.2%, which is the top value reported for All-PSCs to date.

It has been suggested that suitable phase separation and good interpenetrating network structure between polymer donors and polymer acceptors can reduce bimolecular recombination and improve All-PSCs efficiency.[16] Due to the entanglement of the polymer chain and the low mixing entropy, the domain size of phase-separated domain structures of the active layer with bulk heterojunction in All-PSCs is often much larger than that of fullerenes-based PSC and small molecules-based PSC.[17] In addition, the charge transfer efficiency of All-PSCs is mainly determined by molecular stacking structure and the orientation of the long polymer chains.[18] Thus, aggregation and crystallization behavior of conjugated polymers play crucial roles in determining the performance of All-PSCs.[19] As illustrated in Figure 1A, molecular orientation is a crucial factor that determines the free charge carrier generation and transport. Generally, face-on orientation with respect to the substrate and donor: acceptor interface is a highly favorable type of orientational texture for efficient charge separation and transport. The mixing behaviors of polymer donor and polymer acceptor are widely described by Flory–Huggins solution theory.[21] Based on this theory, Figure 1B,C also give the thermodynamic phase diagrams of all-polymer blends with symmetric and asymmetric molecular

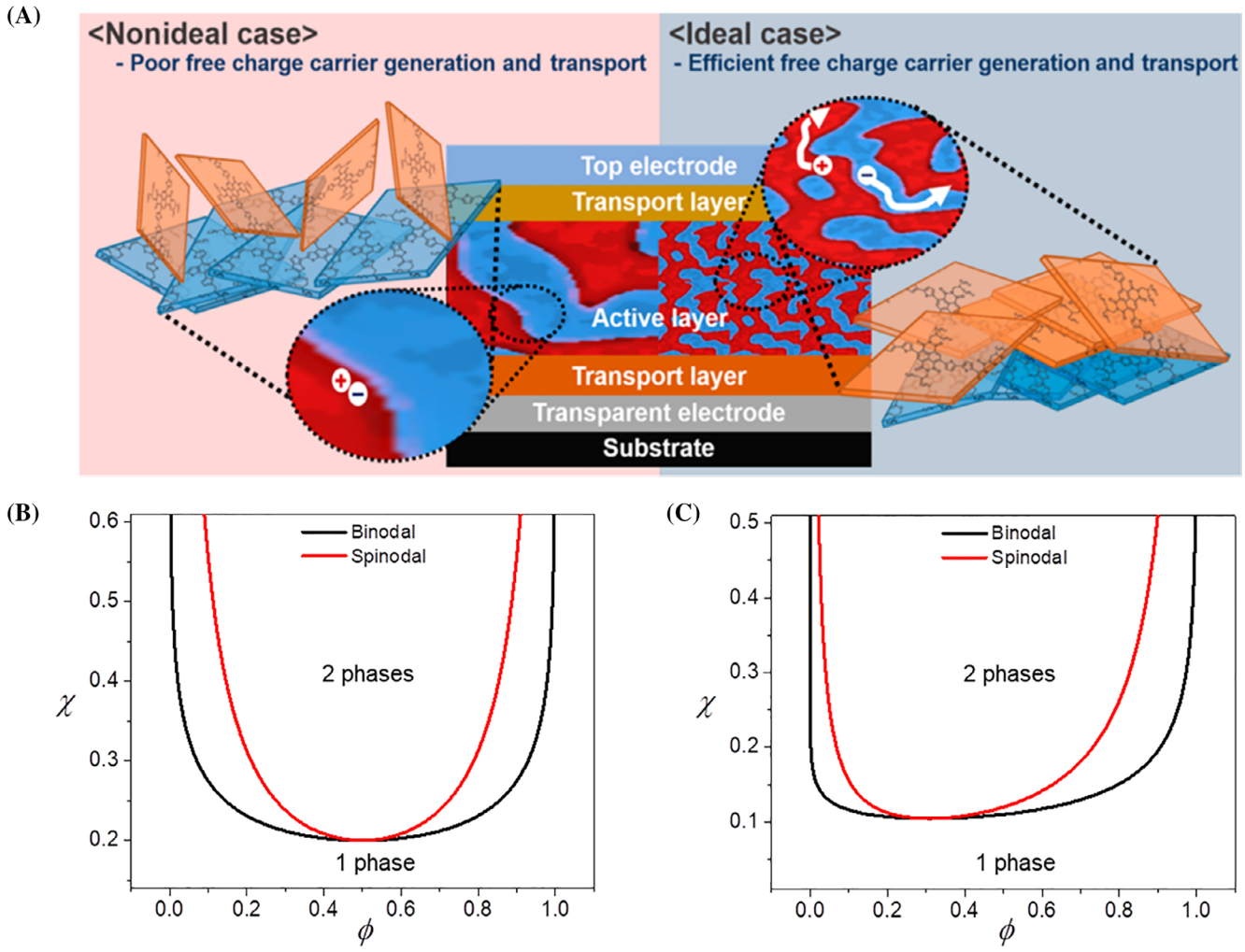

FIGURE 1 (A) Schematic Illustration of all-polymer solar cells with ideal and nonideal morphologies. Reproduced with permission.[20] Copyright 2016, American Chemical Society. Phase diagrams of all-polymer blends with symmetric molecular weights (B) and asymmetric molecular weights (C)

weights. In the phase diagrams, one phase and two phases regions are separated by the binodal curves. Systems that fall in the two phases region favor phase separation while the regime below the binodal curve corresponds to a homogeneous state without any phase demixing. To rational control the morphology, the phase-separated structures should be understood in the context of thermodynamics and kinetics.[21]

In recent years, researchers have made extensive efforts to control and optimize the morphology of polymer blends for high-performance All-PSCs. For instance, lots of studies have reported that the molecular weight of polymer donors and polymer acceptors play important roles in governing the photovoltaic properties of All-PSCs.[2] Exploring optimal D:A to form a suitable phase separation structure is conducive to the generation and diffusion of excitons. The molecular weight of polymer has an important effect on the aggregation tendency, phase separation, and main chain orientation.[22] Active layer processing and engineering are common and facile means to improve blend film morphology.[23] The spin-coated films processed with a single solvent often show poor morphology (such as increased phase separation, decreased ordering of polymer chains, and phase purity) and undesirable photovoltaic performance.[24] Fortunately, solvent engineering, additive engineering, thermal annealing, and solvent vapor annealing can effectively optimize the morphology of the blended film.[25] In addition, one can adjust the side chains and regioregularity of the polymers to effectively control their conformation, orientation, and stacking.[26]

In this article, we are going to assess the pivotal studies on promoting All-PSCs performance via morphology control over the past decade (2011–2021). In particular, the understanding of commonly used NDI-based acceptor polymers and the newly emerging polymerized nonfullerene small molecule acceptors[27] are discussed in detail. Importantly, we describe some of the typical strategies for controlling morphology in detail and summarize the structure-performance relationships of All-PSCs through reports in recent years. Finally, we discuss the present challenges in manipulating the film morphology of All-PSCs and provide an outlook on the future directions and opportunities in this exciting arena of All-PSCs.

2 | NDI-BASED POLYMER ACCEPTORS

2.1 | NDI-based polymer acceptor-N2200

In the past decade, a variety of polymer acceptors based on different building blocks have been developed.[5,9,28–32] Conjugated polymers based on NDI are used as polymer acceptors in All-PSCs. Among these, P(NDI2OD-T2),[33] broadly known as N2200, is the most widely used polymer acceptor to date due to the excellent electron affinity and electron transport performance of the NDI unit. In the recent decade, All-PSCs based on N2200 have developed rapidly and have achieved PCEs in excess of 11% (Table 1).

Regioregularity and molecular weight are crucial factors that determine the crystallinity and orientation textures of polymer acceptors.[2–4] The regioregularity effect of N2200 was discussed at length in Neher's report.[2] Their GIWAXS characterization of the regioregular N2200 films revealed that the casting solvents have a profound impact on the molecular orientation of the polymer chains with respect to the substrate. In terms of molecular weight, Marks and colleagues[49] proposed an optimization matrix strategy in All-PSCs performance by systematic molecular weight modulation of both polymer donor and polymer acceptor. In the study, they systematically investigated the influence of the molecular weight on the blend film morphology and photovoltaic performance of All-PSCs composed of the polymer donor PTPD3T and polymer acceptor N2200. Experimental and coarse-grain modeling results revealed that systematic variation of polymer molecular weight significantly impacts both intrachain and interchain interactions, which ultimately determines the degree of phase separation and morphology evolution. Importantly, the strategy of the 2D molecular weight optimization matrix can identify a PCE "sweet spot" at intermediate molecular weights of both polymer donor and polymer acceptor (see Figure 2A–C). These results highlighted the crucial need for a balanced aggregation strength between the polymer donor and polymer acceptor to achieve high-performance All-PSCs with optimal morphology. Proper and precise tuning of the molecular weights of both donor and acceptor polymer should not be ignored.

One of the extensively studied All-PSCs systems is P3HT:N2200. In 2012, Neher et al.[50] compared All-PSCs comprising two different low-bandgap NDI-based copolymers, namely N2200 and P(NDI-TCPDTT), as acceptors and regioregular P3HT as the donor. They found that these naphthalene copolymers have a strong tendency to pre-aggregate in certain solvents, and the preaggregation of polymer acceptors can be completely suppressed by using solvents with large and polarizable aromatic cores. All-PSCs prepared from these nonaggregated polymer solutions yielded dramatically increased PCEs of 1.4%. The optical analysis revealed that the degree of polymer aggregation in the solid P3HT:N2200 blends anti-correlated with their photovoltaic performance. Scanning near-field optical microscopy (SNOM) and AFM

TABLE 1 Photoactive blend compositions and operating metrics of recent N2200 based All-PSCs

Acceptor	Donor	Architecture	V_{oc} (V)	J_{sc} (mA cm^{-2})	FF (%)	Highest PCE (%)	Year (Refs.)
P(NDI2OD-T2)	P3HT	Binary	0.52	1.41	29	0.21	2011[29]
P(NDI2OD-T2)	PTB7	Binary	0.799	6.28	53	2.66	2014[1]
P(NDI2OD-T2)	PTQ1	Binary	0.84	8.85	55	4.1	2014[34]
P(NDI2OD-T2)	PTB7-Th	Binary	0.821	10.61	53	4.60	2014[35]
P(NDI2OD-T2)	NT	Binary	0.77	11.5	56	5.0	2014[36]
P(NDI2OD-T2)	PBDTTT-EF-T	Binary	0.794	13.0	55.6	5.73	2014[37]
P(NDI2OD-T2)	PPDT2FBT$_H$	Binary	0.85	8.98	47	8.74	2015[38]
P(NDI2OD-T2)	J51	Binary	0.83	14.18	70.24	8.27	2016[39]
P(NDI2OD-T2)-H	TQ-F	Binary	0.84	13.61	63.9	7.31	2016[3]
P(NDI2OD-T2)$_{HW}$	PTzBI	Binary	0.86	15.97	63.47	8.72	2017[12]
P(NDI2OD-T2)	PTzBI-Si	Binary	0.865	15.76	73.76	10.1	2017[40]
P(NDI2OD-T2) + PNTB	PBTA-BO	Ternary	0.84	15.77	74.9	10.09	2018[41]
P(NDI2OD-T2)	PBTA-BO + PTzBI-Si	Ternary	0.836	15.64	77.92	10.12	2018[42]
P(NDI2OD-T2)	PTzBI-Si	Binary	0.85	16.	77.9	11.0	2019[43]
P(NDI2OD-T2)	PTzBI-Si$_H$	Binary	0.85	17.2	77.9	11.5	2019[44]
P(NDI2OD-T2)	J51 + PTB7-Th	Ternary	0.81	17.37	63.7	9.29	2019[45]
P(NDI2OD-T2)	PTzBI-Si	Binary	0.88	17.62	75.78	11.76	2019[46]
P(NDI2OD-T2)	P-EH	Binary	0.94	12.37	64	7.47	2020[47]
PNDI-2FT-0.1	PBDB-T	Binary	0.85	16.62	67.1	9.46	2021[48]

characterizations indicated that films with a high degree of aggregation formed large-scale pure donor and acceptor domains. As such, the intermixing of the donor and acceptor components can be improved by suppressing the aggregation of N2200 at the early stage of film formation. Later on, they further correlated the morphology with bimolecular recombination by investigating the role of solvent additive.[51] From the perspective of thermodynamics, Loo et al.[52] revealed that altering the polymer: solvent interaction is able to tune the morphology of P3HT:N2200 based All-PSCs. Han et al.[53] employed in situ temperature-resolved GIWAXS to study the molecular orientation and phase separation of the P3HT:N2200 blend in step-by-step heating and cooling processes. They found the interpenetrating network of P3HT:N2200 forms during the crystallization process of the polymers. It was found that P3HT crystallizes with edge-on orientation, while N2200 crystallizes with face-on orientation. By fabricating P3HT/N2200 bilayers at various conditions, Ma et al.[54] were able to clarify the role of molecular orientation in determining V_{oc} of All-PSCs.

Polymer donors play an equally important role with polymer acceptors in the morphology optimization of All-PSCs. In comparison with P3HT, a benzodithiophene-based low bandgap polymer PTB7 boosted the PCE of All-PSCs up to 2.7%.[1] This work inspired intensive research interest in applying new polymer donors.[34,36,38,47,55,56] For instance, Kim et al.[57] studied the phase separation behaviors of PDFQx3T:N2200-based All-PSCs by varying the film-processing solvents (chloroform, chlorobenzene, *o*-dichlorobenzene, and *p*-xylene). The different volatility and solubility of the casting solvents greatly impact the aggregation of the polymers and their blend morphology. The domain sizes were tuned in the range of 30–300 nm and well correlated with the J_{sc} of the devices. Owing to the large interfacial areas and efficient exciton separation, All-PSCs with the smallest domain size of ~30 nm in the active layer (using chloroform) produced the highest J_{sc} and PCE of 5.1%. Woo and Kim et al.[38] prepared three batches of a polymer donor PPDT2FBT with different number-average molecular weight values of 12 kg mol^{-1} (PPDT2FBT$_L$), 24 kg mol^{-1} (PPDT2FBT$_M$), and 40 kg mol^{-1} (PPDT2FBT$_H$) to demonstrate how the molecular weight of polymer donor affects the degree of phase separation and the PCE of All-PSCs (see Figure 2D). Combining RSoXS, GIWAXS, and AFM analysis, they found that the phase separation behavior in the PPDT2FBT:N2200 blend highly depends on molecular

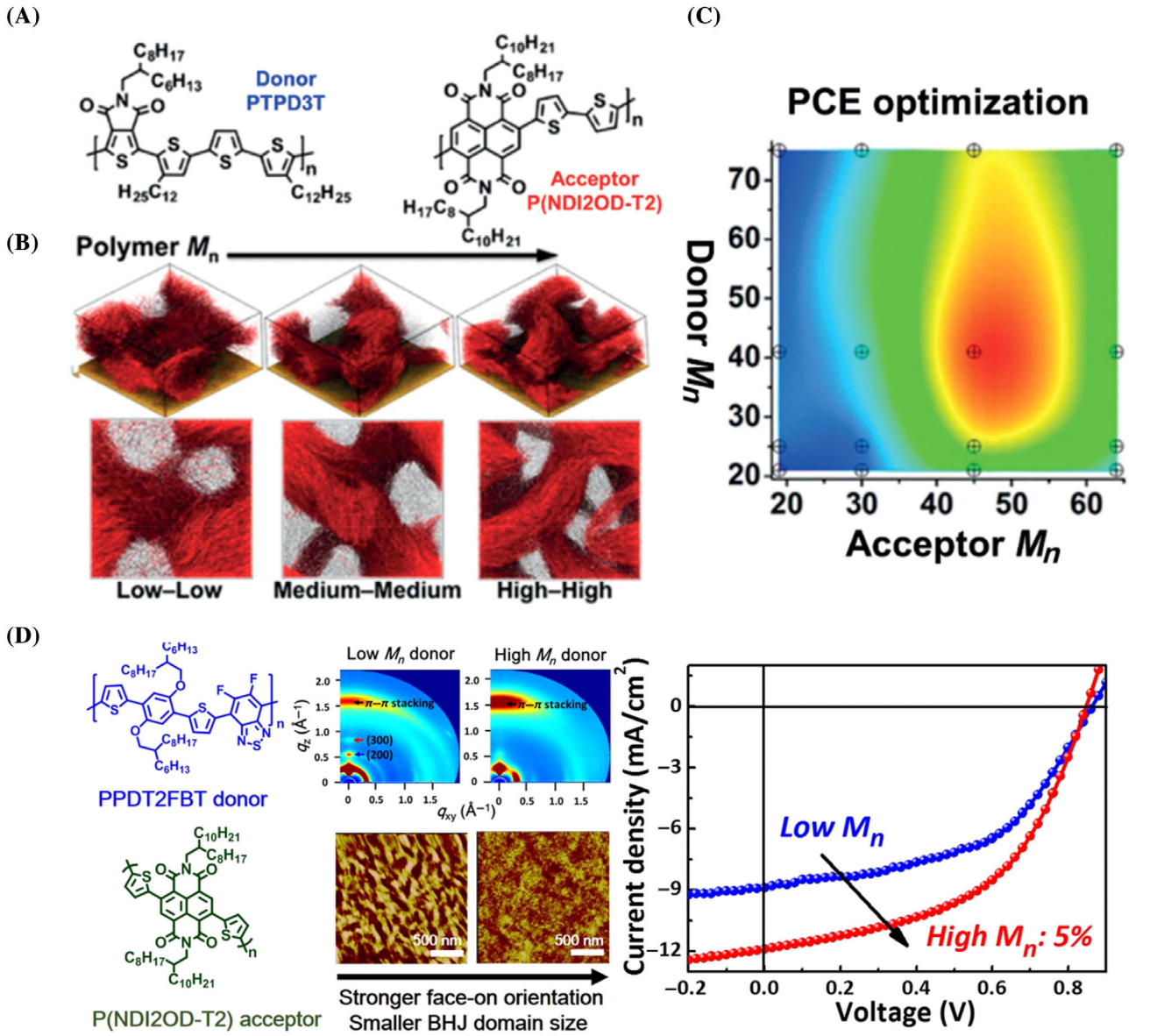

FIGURE 2 (A) Chemical structures of the PTPD3T and N2200. (B) Coarse-grain modeling of the phase separation process as a function of the polymer molecular weights. (C) 2D plots of device power conversion efficiency as a function of the polymer molecular weights. Reproduced with permission.[49] Copyright 2016, American Chemical Society. (D) GIWAXS patterns, AFM height images, and *J*–*V* curves of PPDT2FBT:N2200 blends as a function of molecular weight of PPDT2FBT. Reproduced with permission.[38] Copyright 2015, American Chemical Society

weight, and the domain size of the PPDT2FBT:N2200 blend film was dramatically reduced from 225 to 115 nm with increasing molecular weight. Thus, the high molecular weight blend exhibited a much better degree of intermixing, while excessively large domains were formed in the low molecular weight blend. As a result, the highest intermixing of high molecular weight PPDT2FBT and N2200 with the smallest domain size contributed to the best PCE of 5.1%.

Interestingly, a common feature of high-efficiency All-PSCs is the utilization of polymer donors with bulky pendant groups (e.g., thiophene or phenyl) in the side chains.[58–60] Here, we will focus on the studies on the aggregated structure of N2200 blended with these representative donor polymers include PTB7-Th, PBDTTPD, J71, PBDB-T, and PTzBI-Si. Simply replacing PTB7 with PTB7-Th resulted in a doubling of solar cell efficiency.[37,61] Kim et al.[35] found that the incorporation of DIO can tune the degree of crystallinity and molecular orientation of N2200, affording remarkable enhancement of electron mobility and J_{sc} in the PTB7-Th:N2200 devices. Wang et al.[13] studied the molecular weight

dependence of morphology and performance of this blend system. They pointed out that the computed average distance between PTB7-Th and N2200 correlates well with J_{sc}. As a result, the distance can be used as an index for predicting the intermixing trends of all-polymer blends. Importantly, these results also emphasized that blend morphology can be tuned via both donor and acceptor polymer aggregation. Park and collaborators[62]

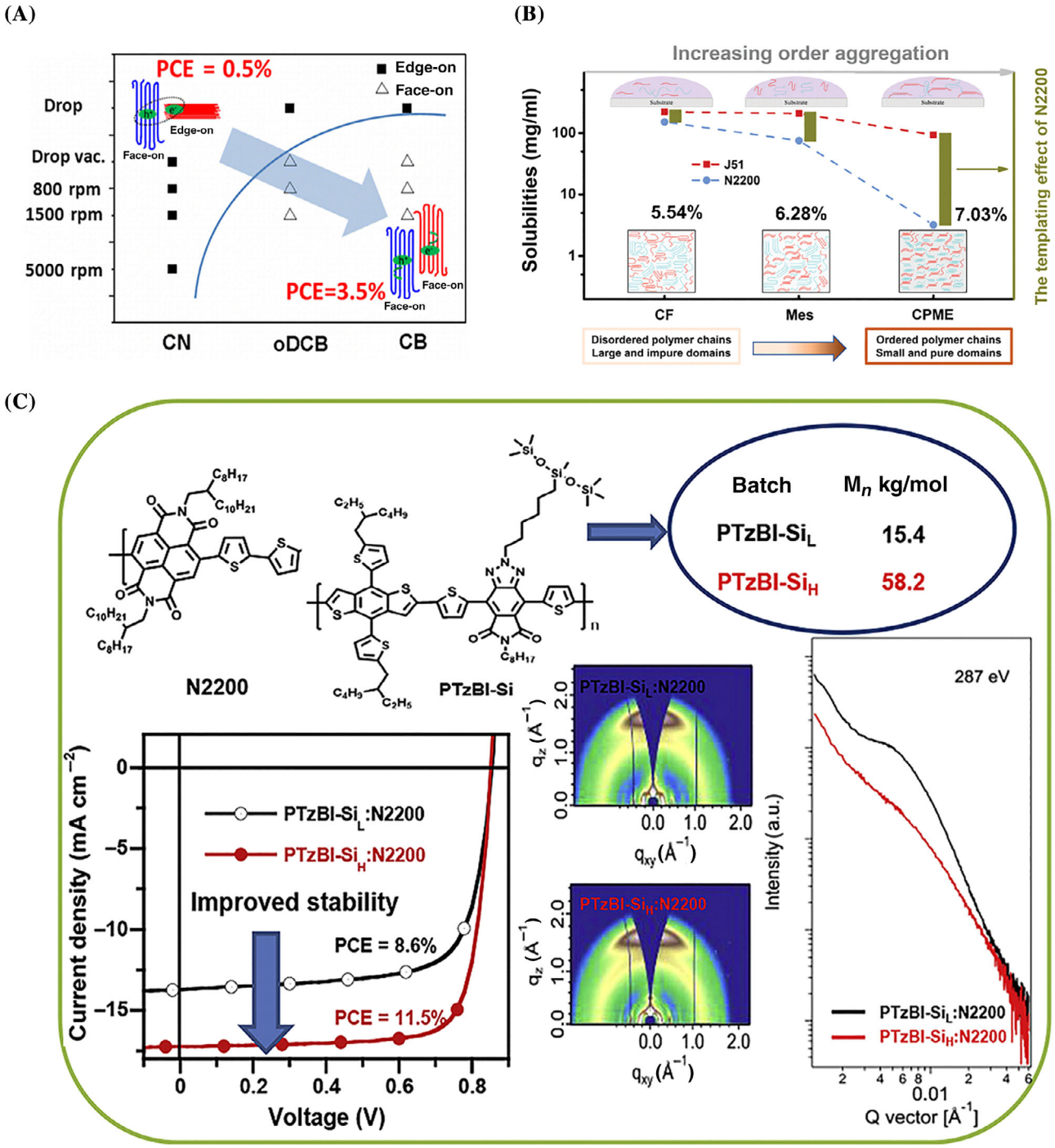

FIGURE 3 (A) Plot of power conversion efficiency and molecular orientation with casting solvent of the PTB7-Th:N2200 blends. Reproduced with permission.[63] Copyright 2015, American Chemical Society. (B) Schematic diagram representing the role of solution-state ordered aggregation of both polymer donor and polymer acceptor in suppressing the liquid–liquid phase separation and improving phase purity by inducing nucleation during the formation of J51:N2200 blend films. Reproduced with permission.[17] Copyright 2019, Royal Society of Chemistry. (C) Effect of molecular weight of PTzBI-Si on the performance and morphology of the PTzBI-Si:N2200 blend films. Reproduced with permission.[44] Copyright 2019, Elsevier

proposed the use of a pentafluorobenzene-based additive (PFE) to tune the morphology via quadrupolar electrostatic interactions between PTB7-Th and N2200. As resolved from AFM, GIWAXS, and near-edge X-ray absorption fine-structure spectroscopy, a favorable interpenetrating morphology with small scale phase separation and enhanced π-π stacking with face-on orientation were achieved in the FPE processed films. These morphology features resulted in an increase in the All-PSCs performance. As depicted in Figure 3A, Han et al.[63] studied the molecular orientation of PTB7-Th:N2200 by grazing incidence X-ray diffraction. They found that CB processed film possessed more favorable face-on orientation and significantly improved PCE, which is 7-fold of that obtained by applying CN.

To further boost the efficiency of N2200 devices, Ye and Hou et al.[58] proposed the use of polymer donors with conjugated side chains to optimize the molecular orientation in All-PSCs. Their polarized RSoXS results showed that PBDB-T:N2200 blends formed a more favorable molecular orientation with respect to the D/A interface, while the polymer without conjugated side chains (i.e., PBDB-O) exhibited edge-on dominated orientation and much poor performance. They further increased the device performance to ∼7.1% by incorporating a trace amount (0.5% by volume) of DIO.[64] PBDB-T:N2200, and thus becoming a model all-polymer system of interest.[22,65–67] Liu et al.[66] recently achieved a high PCE of ∼7.8% by applying sequential crystallization of the polymer donor and polymer acceptor to decrease the domain size of PBDB-T:N2200. In the meanwhile, the crystallinity and molecular orientation were also optimized. The relationships among crystallization kinetics, morphology, and device performance were also established. In addition, the PBDB-T:N2200 blend system exhibited excellent PCE tolerance to blend-ratio changes and excellent long-term stability against oxygen and moisture, as shown by Ma and coauthors.[22]

Other polymer donors demonstrated good performance with N2200. Particularly, poly(benzodithiophene-alt-benzotriazole) derivatives are also widely used donor polymers in high-performance All-PSCs.[68] In 2016, the Li group proposed the use of a fluorinated medium bandgap benzodithiophene-alt-benzotriazole copolymer J51 with N2200, which exhibited a high PCE of 8.27%, mostly benefiting from the complementary absorption in the vis–NIR region of 300–850 nm, matched energy levels, and phase-separated interpenetrating network.[39] Han et al.[17] selected chloroform (CF), mesitylene (Mes), and cyclopentyl methyl ether (CPME) to manipulate the domain size and phase purity of J51:N2200 blends by promoting the solution ordered aggregation and the confinement of acceptor N2200 to J51 during phase separation (see Figure 3B). The blend film processed with CPME exhibited a small domain size (∼20 nm), interpenetrating network structure, and a higher degree of crystallinity. This optimized morphology enabled the highest PCE. Following this work, they further paired a miscible donor blend (J51 and PTB7-Th) with N2200.[45] Owing to the reduced competitive effect of intermolecular interactions, the constructed ternary films featured a morphology of uniform phase demixing. It was found that PTB7-Th acts as a crystallization regulator to enhance the face-on orientation in ternary blend films. The ternary All-PSCs showed a high PCE of 9.6% when CPME was used as the processing solvent, with the PTB7-Th content holding a 30% weight ratio in polymer donors. The results suggest that the photovoltaic performance of many All-PSCs can be further improved by fine-engineering the domain size, domain purity, and polymer packing.

The most prominent combination among the polymer:N2200 systems is PTzBI:N2200, pioneered by Huang and Ying et al.[44,69] The team did a series of studies to understand the aggregated structure of PTzBI:N2200 and its derivatives.[12,41,42,44,70–72] In 2017, a high PCE of 9.16% was achieved in PTzBI:N2200-based all-PSCs by selecting an environmentally friendly solvent MeTHF to process the all-polymer layer.[12] MeTHF affords a preferable film morphology than commonly used solvents such as CB. By blending a sensitizer polymer PBTA-BO with PTzBI:N2200, they achieved a record high FF over 0.78 and a remarkable PCE over 10%.[42] The PCE of the PTzBI:N2200 binary blend was improved to 10.1% by incorporating an alkyl side chain terminated with a 1,1,1,3,5,5,5-heptamethyltrisiloxane into the triazole moiety of PTzBI.[40] The improved efficiency was induced by favorable face-on orientation and high crystallinity, as well as high and balanced charge mobilities. They also investigated the effect of molecular weight of the resultant polymer PTzBI-Si on the morphology and performance of the PTzBI-Si:N2200 blend.[44] As depicted in Figure 3C, the high molecular weight batch exhibited higher PCE (up to 11.5%) and stability than the low molecular batch in All-PSCs devices. The team also reported that the performance of All-PSCs based on the PTzBI-Si:N2200 blend could be boosted to 11% by applying another green solvent system based on CPME.[43] In 2019, Liu and collaborators[46] employed PTzBI-Si:N2200 as the active layer and achieved a high PCE of 11.76%, which is the highest ever reported for N2200-based All-PSCs. The polymer blend films were processed with MeTHF and prepared by slot die printing. In contrast, All-PSCs devices processed by high-boiling point chlorobenzene delivered a rather poor PCE of less than 2%. By combining GIWAXS and RSoXS techniques, they

revealed that low boiling point (volatile) solvent could quickly freeze the morphology. Further, the solubility limit of PTzBI-Si and N2200 in MeTHF facilitates the formation of a multi-length scale morphology, which well explains the excellent performance.

2.2 | Other NDI-based polymer acceptors

Beyond N2200, other NDI-based acceptors also showed promising performances.[73–84] To optimize the performance of NDI and bithiophene-based copolymer

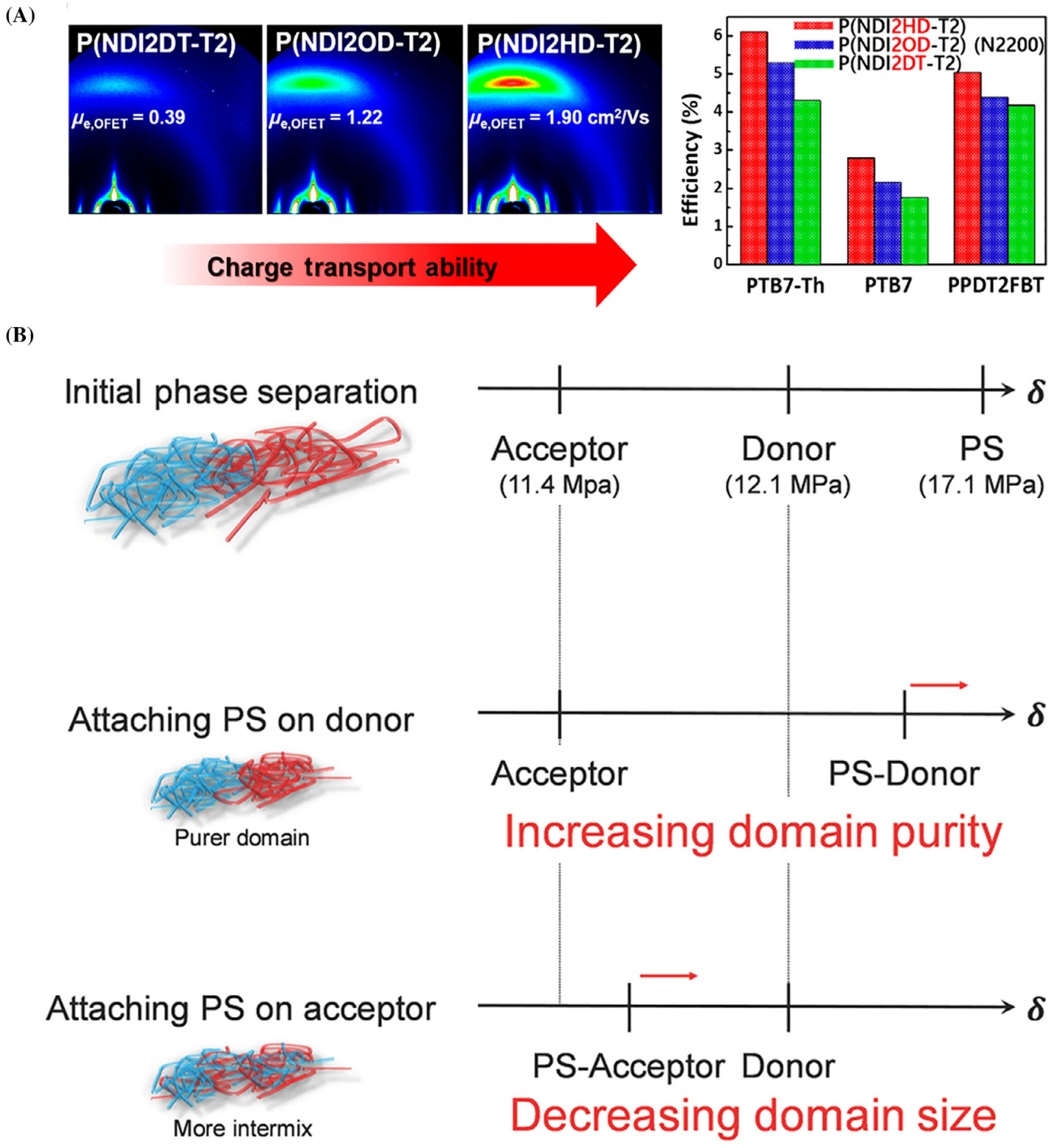

FIGURE 4 (A) Two-dimensional GWAXS patterns of the pristine P(NDI2HD-T2), P(NDI2OD-T2) (N2200), and P(NDI2DT-T2) films. PCEs of all-polymer solar cells were obtained by blending the acceptors with PTB7-Th, PTB7, and PPDT2FBT, respectively. Reproduced with permission.[85] Copyright 2016, Wiley. (B) Schematic illustration of the phase separation behavior in the blend films of polymer donor and acceptor (with or without PS attached to the side chains) and the hypothetical order of solubility parameter of each polymer. Reproduced with permission.[86] Copyright 2017, Wiley

acceptors, Kim et al.[85] varied the alkyl chain of P(NDI2OD-T2) (N2200) as depicted in Figure 4A. The comparative study shows that the crystallinity highly depends on the alkyl chains. Among these three acceptors, P(NDI2HD-T2) exhibited more pronounced crystallinity than N2200 and P(NDI2DT-T2), thereby resulting in superior 3D charge transport and the best PCE in All-PSCs irrespective of the polymer donors. The molecular weight effect of P(NDI2HD-T2)[87,88] on the packing structures and orientations, charge transport properties, and photovoltaic performances in All-PSCs were also studied.[89] An interesting transition in the polymer orientation from edge-on to face-on was realized by simply increasing the molecular weight of P(NDI2HD-T2). Using a set of NDI and thiophene copolymers named PNDIT-R with three different side chains, that is, 2-hexyldecyl (HD), 2-octyldodecyl (OD), and 2-decyltetradecyl (DT), Kim et al.[90] also highlighted the significance of engineering alkyl side chains of the polymer acceptor for producing highly efficient All-PSCs. Among the three polymers, PNDIT-HD was proven to be the best one for promoting face-on orientation and finely phase-separated domains. They further demonstrated the use of a highly crystalline small-molecular additive, 6,6′-dithiopheneisoindigo (DTI) 91 to blend the morphology and crystalline packing structures of polymers, which resulted in better performance in All-PSCs. It was revealed that a small amount of DTI improves the polymer crystallinity without causing phase separation in the all-polymer blends. In addition, the branching point of the side chains in NDI units of polymer acceptors also has a profound impact on the polymer crystallinity/orientation and domain size in all-polymer blends.[92]

Gaining control over the self-assembly of polymer acceptors via molecular design to manipulate blend morphology is quite challenging in the field. Wang et al.[93] reported a facile method to modulate the crystallinity of N2200, by designing a series of random polymers PNDI-T*x*, where a certain amount of bithiophene in the N2200 backbone was replaced with thiophene (*x* is the percentage of thiophene). It was found that the acceptor PNDI-T10 is properly miscible with PTB7-Th. With the assistance of solvent annealing, the PTB7-Th:PNDI-T10 devices achieved a high FF of 0.71 and PCE of 7.6%, which is significantly higher than that of the control PTB7-Th:N2200 cells. Large-area devices based on PTB7-Th:PNDI-T10 reached a PCE of 6.65%, which was also the highest value for flexible ITO-free All-PSCs.[94] Alternatively, Cao et al.[95] developed a series of N2200 derived random copolymer acceptors NOEx, where x is the percentage of linear oligoethylene oxide chain substituted NDI units relative to total NDI units. Notably, NOE10 afforded a much higher PCE of 8.1%, with a record high FF of 0.75 in All-PSCs. Bao et al.[86] proposed the use of oligomeric polystyrene (PS) side chain to tune the phase separation of All-PSCs. As shown in Figure 4B, attaching the PS side chain to the polymer donor likely yields a larger interaction parameter and a higher tendency of demixing, thereby resulting in higher domain purity. Attaching the PS side chain to the polymer acceptor likely yields a smaller interaction parameter and a higher tendency of intermixing, which ultimately forms smaller domains. Most recently, Bao group[96] systematically replaced a certain amount of alkyl side-chains of N2200 with compact bulky side-chains (CBS) and synthesized a series of random copolymer (PNDI-CBS*x*) with different molar fractions ($x = 0$–1) of the CBS units. They found that both solution-phase aggregation and solid-state crystallinity of these polymer acceptors are progressively suppressed with increasing x, as probed by a set of techniques, including UV–vis absorption and photoluminescence spectroscopies, DSC, GIWAXS, and RSoXS. Compared to the highly self-aggregating N2200, more amorphous polymer acceptor enabled All-PSCs with significantly increased PCE up to 8.5%. As evidenced by PL quenching and R-SoXS data, the higher Jsc is ascribed to the smaller acceptor polymer phase-separation domain sizes. On the other hand, the PCE will reduce if the aggregation and crystallinity of the acceptor polymer are weakened too much. In this case, and the highly amorphous polymer acceptors appear to induce the formation of larger donor polymer crystallites and increase the donor phase-separation domain sizes. These studies together demonstrated that random polymerization is a simple yet effective way to modulate the self-aggregation of N2200, and crystallinity/aggregation of polymer acceptors can be fine-tuned by applying random polymerization.

In 2015, Jen group[18] first reported that proper fluorination of N2200 was able to improve its electron-accepting characteristics, crystallinity, and electron transport (Figure 5A). As a result, the derived All-PSCs exhibited a high PCE of 6.29%, which shows a 20% enhancement in PCE compared to the reference cell based on N2200. Further, the fluorinated derivative of N2200 with a longer alkyl chain possessed increased crystallinity and electron-transporting ability. Consequently, a higher PCE of 6.71% was obtained. The study demonstrated that proper fluorination and side-chain engineering of polymer acceptors are facile approaches to optimize the performance of All-PSCs. A comparative study of N2200 and its fluorinated polymer by Kim et al.[16] also demonstrated a similar trend. As shown in Figure 5B, the blend film based on fluorinated N2200 possesses lower roughness and smaller phase size due to the lower interfacial tension, which is beneficial to the

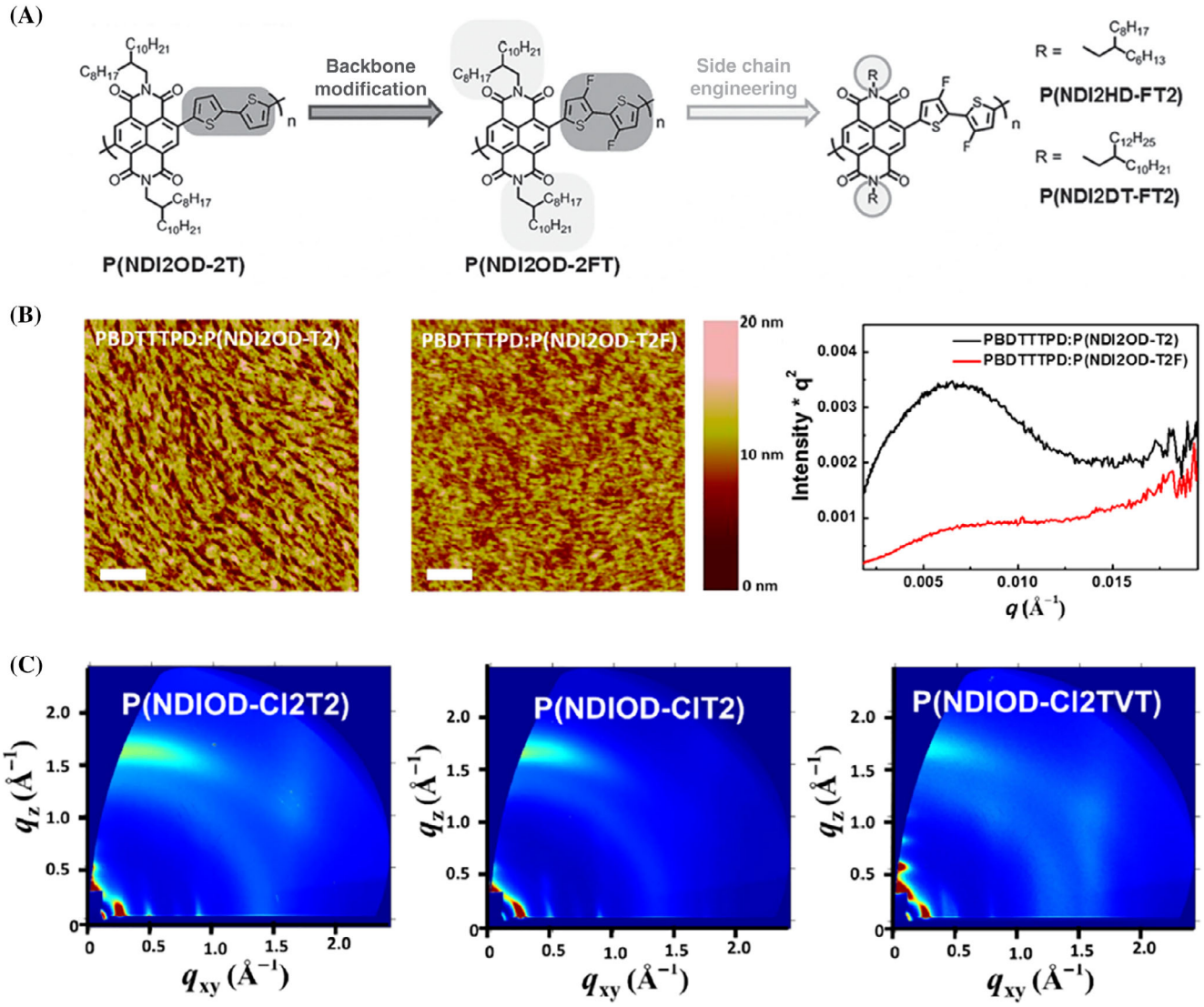

FIGURE 5 (A) Chemical structure of polymer new receptor. Reproduced with permission.[18] Copyright 2015, Wiley. (B) AFM height images and R-SoXS profiles of PBDTTTPD:P(NDI2OD-T2) and PBDTTTPD:P(NDI2OD-T2F). Reproduced with permission.[16] Copyright 2016, American Chemical Society. (C) Two-dimensional GWAXS patterns of P(NDIOD-Cl2T2), P(NDIOD-ClT2), and P(NDIOD-Cl2TVT). Reproduced with permission.[26] Copyright 2020, American Chemical Society

formation of an interpenetrating network. The structural differences caused by fluorination can also be confirmed by the R-SoXS measurement. Recently, the chlorination of N2200 was systematically carried out by Kim et al.,[26] whose research highlighted the effectiveness of controlling the chlorination patterns of polymer acceptors to modulate their aggregation structures and photovoltaic performance. Due to the strong noncovalent interaction of Cl atoms, P(NDIOD-ClT2) shows a stronger tendency to aggregate, face-on ordering (Figure 5C), and higher electron mobility. As a result, P(NDIOD-ClT2)-based All-PSCs achieved a high PCE of 7.22%.

The selection of donor polymers is crucial to the performance enhancement of All-PSCs. Zhou et al.[97] achieved a PCE of 3.6% for All-PSCs by introducing a conjugated side chain into a polymer donor to improve the miscibility of the donor: acceptor blend and by adding small amounts of DIO to increase the aggregation of polymer acceptor PC-NDI. Chen and Zhou et al.[98] reported high-performance ternary All-PSCs by adding the second polymer donor J71 into the PBDB-T:PNDI-2T-TR (5) reference system as a compatibilizer, resulting in a high PCE of >9%. Based on their thermal analysis, J71 and PBDB-T are miscible, which strictly follows the general description of the Fox equation. According to miscibility analysis, the incorporation of J71 not only optimized the in-plane morphology but also induced favorable donor: acceptor distribution in the vertical

direction. This study provided some informative rules to select the appropriate third polymer from the viewpoint of mixing thermodynamics. Staring from PTB7-Th, a regioregular terpolymer[99] was designed to study how its packing structure affects its photovoltaic properties in All-PSCs. The derived terpolymer showed enhanced intermolecular π–π stacking interactions and larger crystallite size, resulting in significantly higher hole mobility and PCE of 6.13% in the All-PSCs devices based on NDI P(NDI2HD–DTAN).

To date, research efforts on these polymer blends have driven the PCEs of N2200-based All-PSCs up to 11.76%[46] for small area devices and over 10%[100] for a relatively large area (1 cm^2), which is on par with that of the state-of-the-art fullerene-based PSCs.[101]

3 | PDI-BASED POLYMER ACCEPTORS

In addition to NDI-based polymers, other types of polymer acceptors have been used for aggregation research in All-PSCs.[102–107]

Perylene diimides (PDI)-based conjugated polymers with high absorptivities, high electron mobilities, and electron affinities on par with those of fullerene acceptors are promising acceptor materials in All-PSCs.[108–110] Early in 2007, PCE of over 1% was first achieved for the blend of PPDIDTT as the polymer acceptor and a bis(thienylenevinylene)-substituted polythiophene (2TV-PT) as the polymer donor. In 2011, Zhou et al.[14] designed six PDI-based polymers by combining PDIs with different donor segments for All-PSC applications. By gradually changing the electron-donating ability of the donor segments, they fine-tuned the physical properties and morphology of PDI-based polymers. The best performance All-PSCs based on PC-PDI reached a high PCE of 2.23%.

In 2014, Bao group[25] proposed a side-chain engineering approach using PS to manipulate the domain size of an all-polymer blend, where a PDI-based polymer P(TP) with a swallowtail alkyl chain substitution was employed as the polymer acceptor. The optimized All-PSCs based on P(TP) as the polymer acceptor reached a high PCE of 4.4%. The length scale of phase separation correlates well with the J_{sc}. In 2015, Jenekhe et al.[111] designed a series of random copolymers based on NDI-selenophene and PDI-selenophene. Their crystallinity and electron mobilities varied with the content of the PDI component (10%, 30%, 50%). In comparison with the reference crystalline NDI-selenophene copolymer (PCE = 1.4%), the new 30PDI with optimal crystallinity yields compatible blends and All-PSCs with enhanced performance (PCE = 6.3%) by blending with the same PBDTTT-CT donor. It is clear that compatibility, blend morphology, and PCE of All-PSCs can be manipulated by molecular design. In 2016, Zhao and coworkers[112] reported a PDI and vinylene alternating copolymer PDI-V with a relatively planar polymer backbone. All-PSCs based on PTB7-Th:PDI-V afforded a high PCE of 7.57% without using any solvent additives or post-treatments. The PCE was the best achieved for All-PSCs based on PDI-based polymers.

Except for variation of the chemical structure, tuning the film formation process is also valuable for obtaining improved performance. In 2014, Cheng and Zhan et al.[113] introduced binary additives, namely a solvent additive DIO and a nonvolatile conjugated molecule PDI-2DTT, to manipulate the morphology of blend films of PPDIDTT and a two-dimensional BDT-based polymer donor PBDTTT-C-T (see Figure 6A,B). In this case, DIO was employed to facilitate aggregation and crystallization of the polymer donor, as well as improve phase separation. As PDI-DTT has a similar structure to that of the polymer acceptor, PDI-2DTT can suppress aggregation of polymer acceptor PPDIDTT. Resulting from the synergistic effects of DIO and PDI-2DTT, suitable phase separation and efficiency enhancement were realized. Later on, they reported a facile strategy of diluting concentrated solution to tune pre-aggregation in solution state and further boosted the performance to >4%.[24]

In 2015, Bao et al.[115] utilized different concentrations of two nonhalogenated additives (1,2,3,4-tetrahydronaphthalene and 1-methyl-naphthalene) to tune the phase separation domain size in the all-polymer hulk heterojunction blend films. By using a volume ratio of 2.0% of 1-methyl-naphthalene, they fabricated over 5% efficiency in All-PSCs with a nonhalogenated solvent system. With the solvent additive presented, the phase separation size can be reduced dramatically. To control the domain size of All-PSCs based on P(TP), They also reported a new approach of flow-enhanced polymer crystallization during solution printing.[96] The patterned coating blades greatly enhanced the nucleation of the polymer donor and reduced the domain sizes. Bao and Gu et al.[116] found that polymers with bulky, irregular PS side chains are more suitable for fine-tuning the size scale of phase separation. Continuously R2R-printed All-PSCs based on the poorly ordered polymer blends reached an impressive PCE of up to 5%.

In 2016, Ye et al.[117] first reported the single benign solvent printing of All-PSCs in ambient air. In a subsequent study,[114] they were able to precisely control the morphological parameters at multiple length scales that formed in printed All-PSCs based on the PBDT-TS1: PPDIODT blend,[118] where the polymeric layers were blade-coated in ambient air. Using RSoXS and GIWAXS

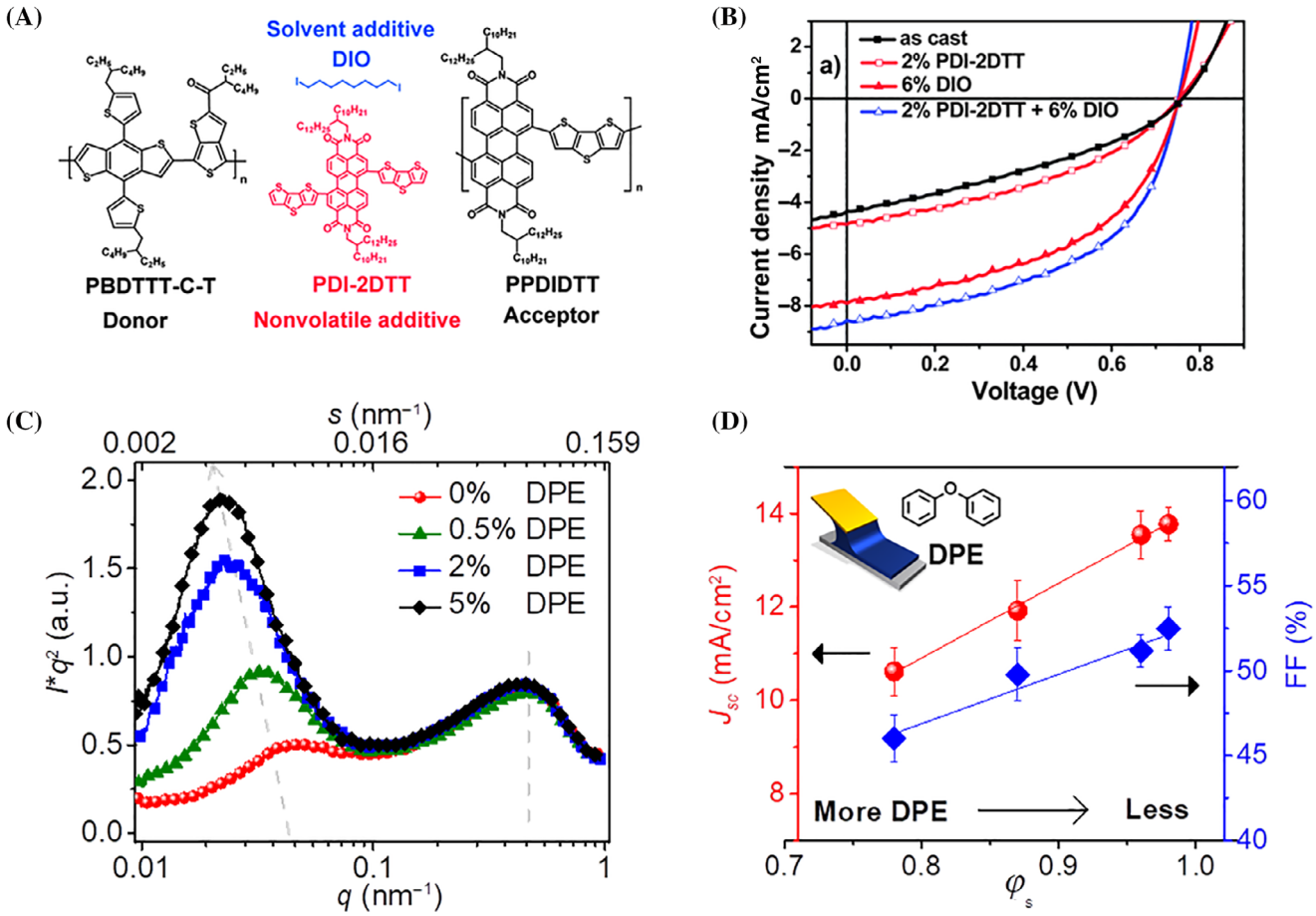

FIGURE 6 (A) Chemical structures of the dual additives and photovoltaic polymers. (B) *J–V* curves of all-polymer solar cells (All-PSCs) with and without additives. Reproduced with permission.[113] Copyright 2014, Royal Society of Chemistry. (C) RSoXS profiles of All-PSCs with different concentrations of DPE. (D) Dependence of J_{sc} and FF in All-PSCs on the DPE concentrations used in the blade coating processing of All-PSCs. Reproduced with permission.[114] Copyright 2017, Wiley

techniques complemented with in-situ spectroscopic ellipsometry, they elucidated how diphenyl ether (DPE), a halogen-free and eco-compatible solvent additive, can precisely control the photovoltaic properties and multilength scale morphologies of the all-polymer blend (see Figure 6C,D). The additive-free All-PSCs printed in the air provided the best PCE of ~5.6%, while the devices with different DPE concentrations are less efficient with some extent of decrease in both J_{sc} and FF observed. The length scales of large domains can be gradually reduced from ~280 to ~140 nm, and the relative volume fractions (φ_s) of small domains gradually increased by decreasing the concentration of the green additive DPE. Both factors well explained the highest photovoltaic parameters observed. Also, the results highlighted that the device performance of printed all-polymer films depends strongly on the characteristics of the smallest domains and demonstrated the benefits of using a single environmentally benign solvent in these All-PSCs.

4 | B ← N AND DPP-BASED POLYMER ACCEPTORS

Most of the polymer acceptors used in All-PSCs are semicrystalline. Conjugated polymers containing the boron-nitrogen coordination bond (B ← N) are amorphous and have emerged as a new class of polymer acceptors in the community[119–121] (examples are shown in Figure 7). To control the aggregation state, Liu et al.[122] optimized the solution preparation method of all-polymer blends (Figure 7A). Unlike the conventional method that polymer donor and acceptor are dissolved together, they first dissolved the polymer donor and acceptor individually and then mixed the two neat polymer solutions immediately before spin-coating, as shown in Figure 7B. In this way, both polymer donor and acceptor have formed aggregates in their individual solutions. When mixed together, the formed aggregates of polymer chains could be largely preserved in blend films after spin-coating. As a consequence, the new method offered improved photovoltaic

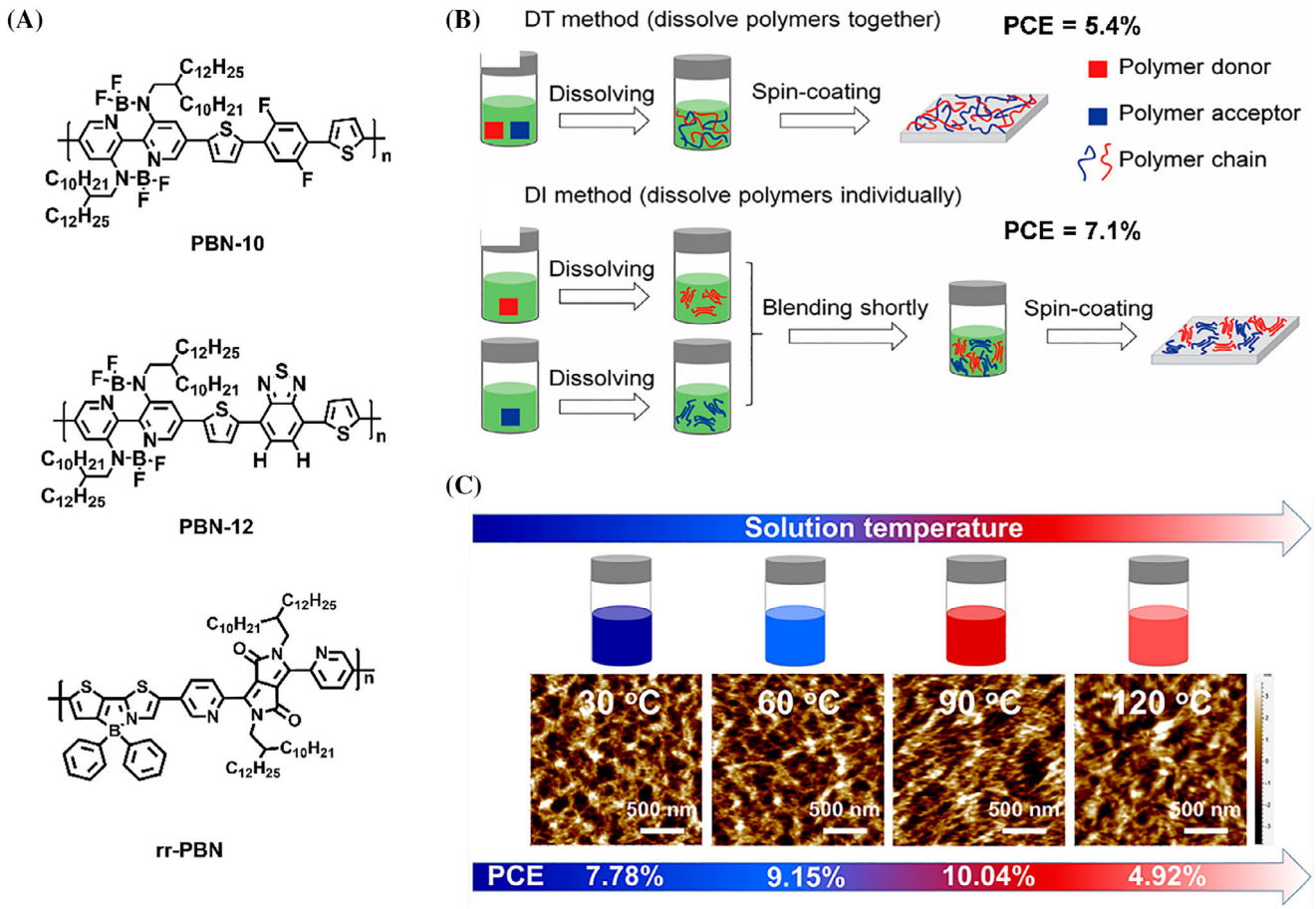

FIGURE 7 (A) Chemical structures of the polymer acceptors containing B ← N units, as discussed in this article. (B) Schematic procedures of DT and DI methods to prepare the blend films for all-polymer solar cells. Reproduced with permission.[122] Copyright 2019, American Chemical Society. (C) Morphology/performance characteristics of all-polymer blend films by varying the solution temperature from 30 °C to 120 °C. Reproduced with permission.[123] Copyright 2020, American Chemical Society

performance due to the improved domain purity and molecular ordering, as exemplified in the study of J61: PBN-10 systems. As a complement to the dissolving together approach, they proposed another method to control the aggregation of polymer donors and acceptors.[123] They studied the aggregation behavior of efficient All-PSCs based on a B ← N unit-based polymer PBN-12 as a function of solution temperature (Figure 7C). They found that promoting the solution temperature can optimize the crystallization degree of polymers and decrease the length scale of phase-separation. The device fabricated with the solution temperature of 90°C exhibited a PCE of over 10%, while the device based on the solution at room temperature obtained a lower PCE of ~7.8%. This study offered a feasible approach to optimize the blend morphology of All-PSCs.

To clarify the role of polymer donor, Liu et al.[124] selected three polymer donors with an identical polymer backbone but different side chains to blend with an amorphous polymer acceptor (rr-PBN). Among the three donors, J91 resulted in the best All-PSCs device performance with the optimal phase separation morphology. This is largely ascribed to the strongest aggregation tendency in solution and moderate crystallinity of J91 film. In comparison, J51 shows the least aggregation tendency in solution and the highest crystallinity in the thin film. The All-PSCs device based on J51 exhibited undesired photovoltaic performance. As a result, the aggregation tendency in a solution of polymer donors plays a dominant role in the phase separation of All-PSCs based on semi-crystalline polymer donor and amorphous polymer acceptor blends. Benefitting from the improved understanding of aggregated structures, the All-PSCs based on a polymer acceptor containing B ← N unit (PBN-10) delivered a high PCE of 27.4% under indoor artificial lighting sources.[125]

The diketopyrrolopyrrole (DPP)-based polymers that possess good structural planarity and crystallinity, high charge carrier mobility, and absorption coefficient have important application potential as acceptor materials of All-PSC.[126–129] In order to obtain deep LUMO level polymer receptors, Janssen et al.[130] have developed conjugated polymers based on electron-deficient DPP units as

polymer acceptors. Combining these DPP acceptors with a DPP polymer donor, they produced All-PSC with a PCE of 0.4%. The low PCE was mainly due to the larger phase separation between the polymers, which led to the decrease of J_{sc}. In 2014, Janssen et al.[131] designed and synthesized a novel polymer acceptor PDPP2TzT based on DPP, which has low-lying HOMO/LUMO levels and high electron mobility. In order to regulate the phase separation, they added 7.5% CN to the solution, which gave a much higher PCE of 2.9%. After that, Janssen[128] and colleagues further evaluated the aggregation structure and photovoltaic properties of All-PSCs prepared by DPP polymers with different thiophene side chains (PDPP2TzT, PDPP2TzBDT, PDPP2Tz2T, and PDPP2TzDTP) as electron acceptors. With the assistance of thermal annealing, solvent engineering, and film thickness optimization, PDPP2TzT exhibited good phase separation and a higher PCE of 3% when the DPP-based polymer acceptor was blended with P3HT.

In addition, Yu et al.[132] found that DPP-based polymer acceptors with alternate structural blocks of different sizes, such as thiophene, benzothiophene, and benzodithiophene, exhibit different aggregation structures and photovoltaic properties due to their different polymerization characteristics. The results show that the large size of the DPP-based polymer receptor has the potential to prepare high-performance All-PSC due to the better miscibility of the polymer system. Long et al.[133] developed a novel polymer receptor with a good absorption coefficient and high electron mobility by copolymerizing BNBP and DPP units. Nanostructures with fibrous aggregates were observed in TEM images of the blend film (PTB7:P-BNBP-DPP), indicating the existence of partial crystallization in the blend film, which is conducive to carrier transport. Recently, Jiang et al.[134] proposed three novel DPP-based polymer acceptors with asymmetric thiophene/benzothiophene side-chain structures (PBTTDPP-BT, PBTTDPP-TT, and PBTTDPP-2FBT). Nanoparticles of several hundred nanometers were found in AFM images of PBTTDPP-2FBT and P3HT blends, which confirmed its better phase separation structure. The All-PSC with P3HT:PBTTDPP-TT and P3HT:PBTTDPP-2FBT afforded PCE of 0.28% and 0.44%, respectively. These results indicate that the modification and optimization of phase separation in DPP-based All-PSC can enhance the charge separation and transport in the active layer and thereby improve the PCE of All-PSC.[135–137]

5 | POLYMERIZED SMALL MOLECULE ACCEPTORS

Another representative and emerging class of polymer acceptors are polymerized small molecule acceptors pioneered by Li and Zhang et al.[27] Starting from an A-D-A-structured nonfullerene small molecule acceptor IDIC-C16, they developed a new polymer acceptor PZ1 with a high absorption coefficient ($>10^5$ cm^{-1}). Matching with star polymer donors such as PBDB-T or its fluorinated version PM6 with large bandgaps, the resulting All-PSCs exhibited high J_{sc} values of 16–17 mA cm^{-2} and PCEs in the range of 9%–11%. In particular, Zhang et al.[23] investigated the effect of CN treatment on the PM6:PZ1 blend film. With the addition of the CN, the optimized blend film showed more ordered packing (higher coherence lengths) of the polymer chains, preferable face-on orientation with respect to the substrate, and more distinct phase separation. These features gave rise to a high PCE of 11.2%. Li et al.[138] recently reported the impact of halogenation (fluorination and chlorination) on IDIC-C16-based narrow bandgap polymer acceptors, namely, PIDIC2T, PIDIC2T2F, and PIDIC2T2Cl (see Figure 8A). Their results indicated that halogen significantly affects the thin-film morphology of the polymer acceptors. By blending with PM6, 5.46%, 4.96%, and 7.11% were achieved for PIDIC2T, PIDIC2T2F, and PIDIC2T2Cl, respectively. This study pointed out the need for backbone halogenation to further improve the performance of All-PSCs. Ying et al.[140] recently also reported a fluorinated polymer acceptor PFA1. The optimized blend films based on PFA1 reached an impressive PCE of 15.11%. Interestingly, this polymer acceptor also afforded high PCEs of ∼12%, ∼13.8%, and ∼14.2% when matched with PTzBI-Si, PM6, and PBDB-T, respectively.

Inspired by the great success of polymerized IDIC-C16 acceptors, Yan group[141] and Zhang group[142] independently reported polymer acceptors PFBDT-IDTIC and PN1, which also enabled over 10% efficiency in All-PSCs. In 2020, the Huang[81] group further used the strategy in developing polymer acceptors based on Y5 as building blocks. By optimizing the molecular weight, the resultant polymer acceptor PJ1 with the highest molecular weight achieved an impressive PCE of 14.4% when matched with PBDB-T. In an independent study, Min et al.[139] demonstrated that the molecular weight of PYT, a structurally similar polymer acceptor of PJ1, is quite sensitive to the photovoltaic performance of PM6:PYT blends. Three batches of PYT were prepared to fine-tune the polymer crystallinity and miscibility with an identical polymer donor PM6. The PYT polymers were designated as PYT_L, PYT_M, and PYT_H from low to high molecular weight. They noted that the PM6:PYT_M device affords the highest PCE of 13.44% for All-PSCs, resulting from the ideal donor: acceptor miscibility (Figure 8B). In contrast, the PM6:PYT_H system exhibited a much poor PCE, which mainly originated from the poor morphology with large domains. In the meantime, Li et al.[143] prepared a series

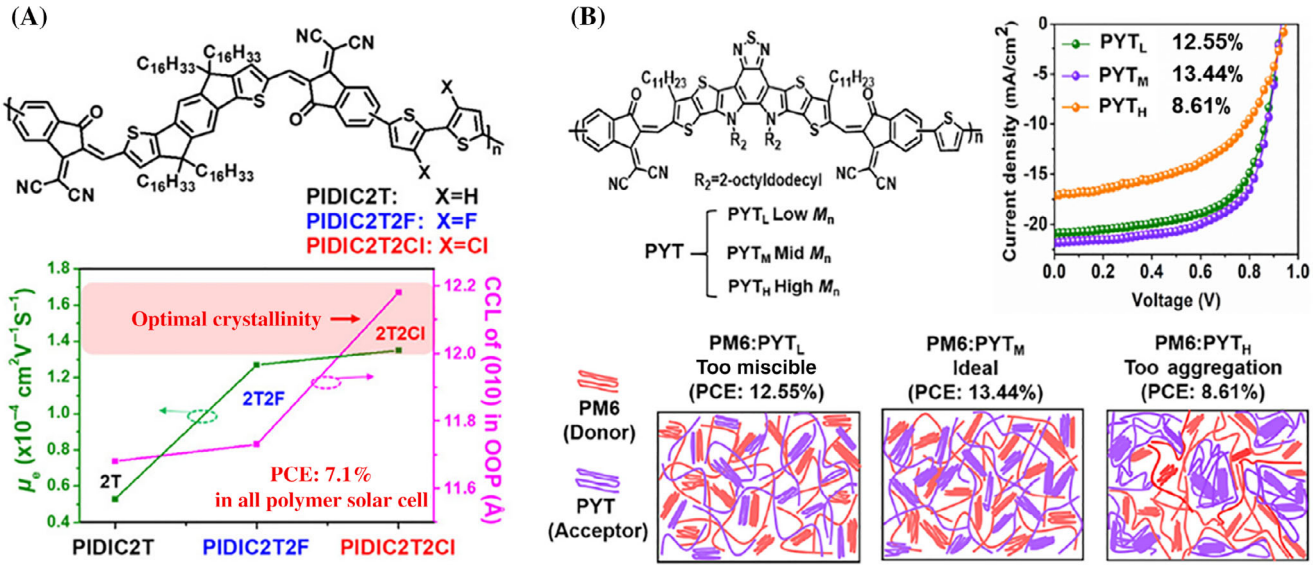

FIGURE 8 (A) Charge transport characteristics and crystallinity in all-polymer blend films based on a set of polymerized small molecule acceptors with varied halogenation. Reproduced with permission.[138] Copyright 2020, American Chemical Society. (B) Typical *J*–*V* characteristics and aggregated structures in all-polymer blend films based on a representative polymerized small molecule acceptor PYT with varied molecular weights. Reproduced with permission.[139] Copyright 2020, Elsevier

of polymerized small molecule acceptors via random ternary copolymerization of a Y6-like unit, thiophene π-bridge unit, and one resultant copolymer achieved the best PCE of over 12.5%.

Most recently, some groups have realized over 15% efficiency in All-PSCs with more desired morphology by further chemically engineering the Y6-based polymer acceptors.[140] For instance, Yan and Min et al.[144] synthesized two regio-regular polymer acceptors (PYF-T-o and PYF-T-m). Strikingly, after the donor polymer PM6 blends, PM6:PYF-T-o forms ordered inter-chain packing and proper phase separation (Figure 9A), which inhibits charge recombination and improves charge transfer efficiency. GISAXS test results show that the size of the phase region of PM6: PYF-T-o is 13.9 nm (Figure 9B), which is consistent with the exciton diffusion length (10–20 nm), while PM6: PYF-T-m is outside this range (24.2 nm). Yang and collaborators[145] successfully prepared two well-regular polymer acceptors with distinct polymerization sites and emphasized that the site of polymerization on small molecule acceptors strongly influences blend morphology and device performance. Due to the balanced charge transfer, favorable morphology, and suitable phase region size (Figure 9C), PM6:PY-IT devices have the highest FF and J_{SC}. The most efficient one achieved the highest PCE of 15.05%. To further improve the performance, Jen et al.[146] developed a regioregular PZT (PZT-γ) to achieve higher regiospecificity for avoiding forming isomers during polymerization. Compared with PZT, the regioregular PZT-γ results in superior backbone ordering and an optimal blend morphology with the donor (Figure 10D), and the PCE of PBDB-T: PZT-γ devices achieved 15.8%.

Besides, doping is a feasible and cost-effective strategy to optimize the performance of a given all-polymer blend system without the sacrifice of aggregated structure. For instance, Peng et al.[150] recently applied a p-doping strategy for two all-polymer blend systems based on a new polymer donor named PNDT-T and a star polymer donor PBDB-T. In both systems, the PCEs are improved substantially upon the p-doping of F4-TCNQ at a trace amount. Moreover, the ternary blend devices based on PNDI-T and PBDB-T reached a significantly improved PCE of nearly 12%. Recently, Min et al.[15] introduced PYT into PM6:PY2F-T as the third component and obtained the highest PCE (17.2%) recorded so far. The research shows that the introduction of PYT polymer acceptor has balanced the degree of phase separation and crystallization, which promotes exciton separation and inhibits carrier recombination. These investigations show that combining the benefits of two well-compatible polymer acceptors with the ternary approach is a simple and reliable strategy to improve the morphology and thus PCE of All-PSCs.

6 | CONCLUSION AND OUTLOOKS

In this article we critically assess the innovative studies on morphology control of All-PSCs and summarize some

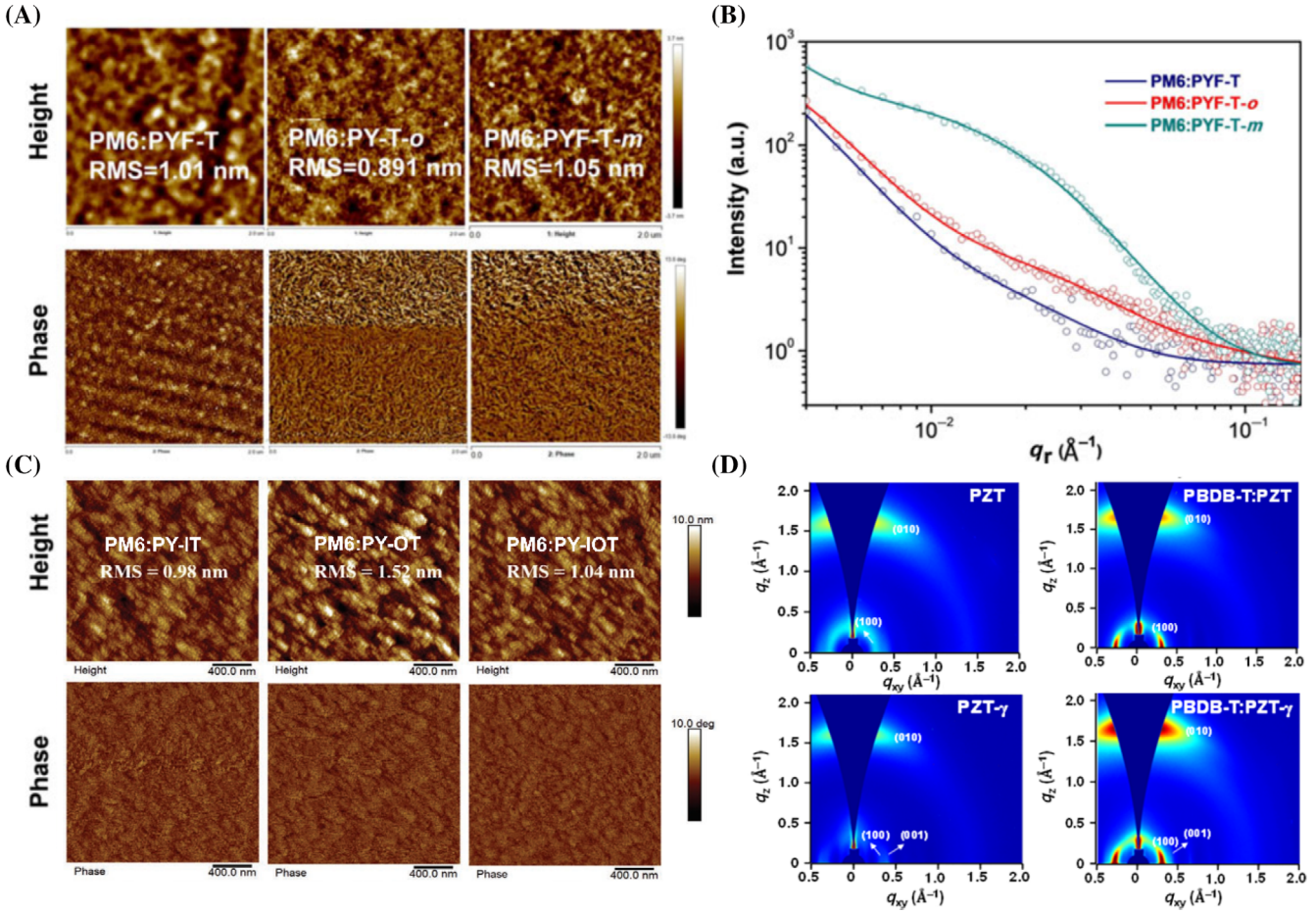

FIGURE 9 (A) The AFM height and phase images, and (B) the GISAXS intensity profiles and fittings along the in-plane direction of the PM6:PYF-T, the PM6:PYF-T-o and the PM6:PYF-T-m blend film. Reproduced with permission.[144] Copyright 2020, Wiley. (C) AFM height images and phase images of PM6:PY-IT, PM6:PY-OT, and PM6:PY-IOT. Reproduced with permission.[145] Copyright 2020, Wiley. (D) 2D GIWAXS patterns of PZT, PBDBT:PZT, PZT-γ, and PBDBT:PZT-γ. Reproduced with permission.[146] Copyright 2020, American Chemical Society

strategies for optimizing the photovoltaic performance of All-PSCs by controlling the thin-film morphology of the blend film. Focused on the NDI-based, PDI-based, DPP-based, B ← N-containing polymer acceptors and polymerized small molecule acceptors, we discussed the key methods for adjusting the aggregated structure of the corresponding blends and optimizing the morphology of films in detail. For all-polymer blends, efforts should be made to fully optimize molecular weight for both polymer donor and acceptor to reach the upper limit of All-PSCs performance with optimal aggregated structure. Furthermore, solvent engineering, thermal annealing, solvent vapor annealing, and coating methods can also effectively optimize the morphology of the blended films.

As illustrated in Figure 10, after a decade of rapid development, the best PCEs of All-PSCs have realized 17%, suggesting that All-PSCs are on the way to catching up with solar cells based on polymer:nonfullerene small molecule blends. Although All-PSCs have made great progress in the last decade, there are still some open questions that have not been well addressed. Here, we propose four possible optimization pathways to further improve the performance and operational stability of All-PSCs.

- **Understanding the synergistic effects of key morphology control methods**

At present, solvent engineering, additive engineering, thermal annealing, and solvent vapor annealing can effectively optimize the morphology of the blend films.[151] The method that works for one system is not necessarily effective for another system. Thus, these optimization methods often need to be carefully and even fully explored.[152–154] In addition, one can adjust the side chains and regioregularity of the polymer to effectively control the conformation, orientation, and stacking of the molecule.[155] However, how to use these strategies in

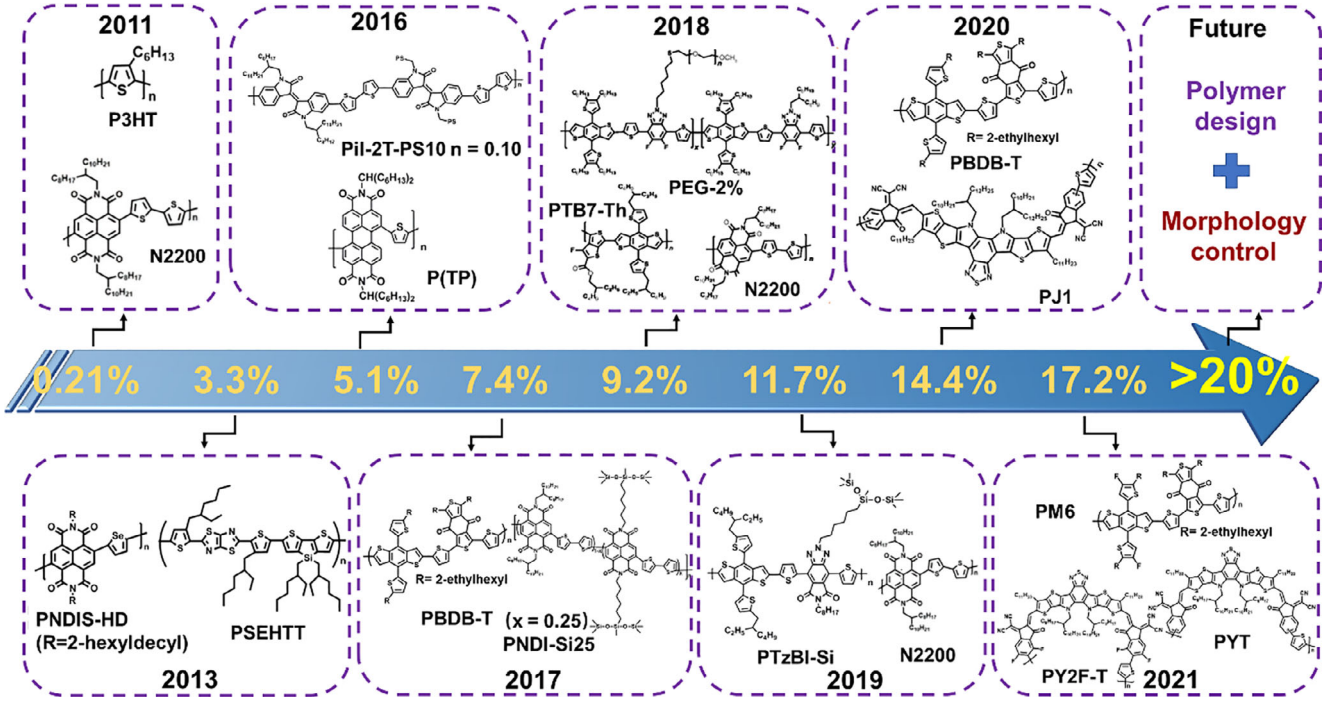

FIGURE 10 The power conversion efficiency development of all-polymer solar cells in the recent decade. The notable active layers include P3HT:N2200,[147] PNDIS-HD:PSEHTT,[73] PiI-2T-PS:P(TP),[115] PBDB-T:PNDI-Si25,[148] PTB7-Th:PEG:N2200,[149] PTzBI-Si:N2200,[46] PBDB-T:PJ1,[81] and PM6:PY2F-T:PYT[15]

a synergistic and elegant way to achieve a win–win situation has not been addressed yet.

- **Introducing advanced tools for the microstructural characterization**

Due to the continued development of advanced tools for precise characterization of soft matters, the aggregation structure and phase behaviors of conjugated polymers have been better understood.[156–158] For instance, the domain size/spacing,[159,160] orientational order,[161,162] and domain purity (composition deviations)[163] of conjugated polymer blends can be analyzed in detail by RSoXS and its associated methods. In addition, cryo-TEM[164] and neutron scattering[165] can greatly assist in monitoring the morphology evolution of polymer blends from solution state to thin-film state. The power of these advanced tools has not been appreciated and accessed by the community well. Undoubtedly, utilizing these advanced techniques will broaden our knowledge of All-PSC morphology.

- **Determining the interaction parameters and molecular miscibility**

As the intrinsic properties of a blended binary system at a given temperature, molecular miscibility has been extensively studied in polymer: small molecule and small molecules-based PSCs by using various experimental techniques.[166–168] The quantitative description of molecular miscibility has promoted the understanding and optimization of these systems based on small molecules, while few studies have been conducted on the molecular miscibility of All-PSCs. Motivated by these previous studies, interaction parameter,[169] a thermodynamic quantity, is expected to play an important role in thermodynamic analysis of All-PSCs.

- **Clarifying the polymer structure- morphology-property relationships**

The film morphology of polymer blends not only affects the PCE of All-PSCs but also closely determines their mechanical property and stability. Revealing the fundamental connections between morphological parameters at different length scales and mechanical parameters[170,171] (elastic modulus, fracture energy, crack-onset strain, cohesion energy, toughness, and so on) warrants in-depth explorations. In future studies, a full set of polymer structure-morphology-property correlations should be further clarified to provide design rules for commercially viable novel All-PSCs.

It is noteworthy that All-PSCs have superior electronic transport properties, mechanical robustness, and stability compared to small molecules-based PSC. In the near future, we anticipate that refining the present

polymer design and morphology control will promote the PCE of the All-PSCs in excess of 20%, leading to rapid commercialization of highly efficient solar cells with large area, high stability, flexibility, and efficiency.

ACKNOWLEDGMENT

Long Ye, Kaihu Xian, and Kangkang Zhou gratefully thank the National Natural Science Foundation of China (No. 52073207), the start-up grant of Peiyang Scholar program from Tianjin University, and the State Key Laboratory of Applied Optics (No. SKLAO2021001A17).

CONFLICT OF INTEREST

The authors declare no conflict of interest.

ORCID

Kaihu Xian https://orcid.org/0000-0001-6929-2871
Long Ye https://orcid.org/0000-0002-5884-0083

REFERENCES

1. Zhou N, Lin H, Lou SJ, et al. Morphology-performance relationships in high-efficiency all-polymer solar cells. *Adv Energy Mater*. 2014;4(3):1300785.
2. Steyrleuthner R, Di Pietro R, Collins BA, et al. The role of regioregularity, crystallinity, and chain orientation on electron transport in a high-mobility n-type copolymer. *J Am Chem Soc*. 2014;136(11):4245-4256.
3. Chen S, An Y, Dutta GK, et al. A synergetic effect of molecular weight and fluorine in all-polymer solar cells with enhanced performance. *Adv Funct Mater*. 2017;27(2):1603564.
4. Choi J, Kim W, Kim S, Kim T-S, Kim BJ. Influence of acceptor type and polymer molecular weight on the mechanical properties of polymer solar cells. *Chem Mater*. 2019;31(21):9057-9069.
5. Ma Y, Zhou X, Cai D, Tu Q, Ma W, Zheng Q. A minimal benzo[c][1,2,5]thiadiazole-based electron acceptor as a third component material for ternary polymer solar cells with efficiencies exceeding 16.0%. *Mater Horiz*. 2020;7(1):117-124.
6. Duan C, Ding L. The new era for organic solar cells: polymer acceptors. *Sci Bull*. 2020;65(18):1508-1510.
7. Benten H, Mori D, Ohkita H, Ito S. Recent research progress of polymer donor/polymer acceptor blend solar cells. *J Mater Chem A*. 2016;4(15):5340-5365.
8. Yin H, Yan C, Hu H, et al. Recent progress of all-polymer solar cells – from chemical structure and device physics to photovoltaic performance. *Mater Sci Eng R Rep*. 2020;140:100542.
9. Wang G, Melkonyan FS, Facchetti A, Marks TJ. All-polymer solar cells: recent progress, challenges, and prospects. *Angew Chem Int Ed*. 2019;58(13):4129-4142.
10. Lee C, Lee S, Kim GU, Lee W, Kim BJ. Recent advances, design guidelines, and prospects of all-polymer solar cells. *Chem Rev*. 2019;119(13):8028-8086.
11. Facchetti A. Polymer donor–polymer acceptor (all-polymer) solar cells. *Mater Today*. 2013;16(4):123-132.
12. Fan B, Ying L, Wang Z, et al. Optimisation of processing solvent and molecular weight for the production of green-solvent-processed all-polymer solar cells with a power conversion efficiency over 9%. *Energ Environ Sci*. 2017;10(5):1243-1251.
13. Wang G, Eastham ND, Aldrich TJ, et al. Photoactive blend morphology engineering through systematically tuning aggregation in all-polymer solar cells. *Adv Energy Mater*. 2018;8(12):1702173.
14. Zhou E, Cong J, Wei Q, Tajima K, Yang C, Hashimoto K. All-polymer solar cells from perylene diimide based copolymers: material design and phase separation control. *Angew Chem Int Ed*. 2011;50(12):2799-2803.
15. Sun R, Wang W, Yu H, et al. Achieving over 17% efficiency of ternary all-polymer solar cells with two well-compatible polymer acceptors. *Joule*. 2021;5(6):1548-1565.
16. Uddin MA, Kim Y, Younts R, et al. Controlling energy levels and blend morphology for all-polymer solar cells via fluorination of a naphthalene diimide-based copolymer acceptor. *Macromolecules*. 2016;49(17):6374-6383.
17. Zhang Q, Chen Z, Ma W, Xie Z, Han Y. Optimizing domain size and phase purity in all-polymer solar cells by solution ordered aggregation and confinement effect of the acceptor. *J Mater Chem C*. 2019;7(40):12560-12571.
18. Jung JW, Jo JW, Chueh C-C, et al. Fluoro-substituted n-type conjugated polymers for additive-free all-polymer bulk heterojunction solar cells with high power conversion efficiency of 6.71%. *Adv Mater*. 2015;27(21):3310-3317.
19. McNeill CR. Morphology of all-polymer solar cells. *Energ Environ Sci*. 2012;5(2):5653-5667.
20. Kang H, Lee W, Oh J, Kim T, Lee C, Kim BJ. From fullerene–polymer to all-polymer solar cells: the importance of molecular packing, orientation, and morphology control. *Acc Chem Res*. 2016;49(11):2424-2434.
21. Song C, Qu Y, Liu J, Han Y. Phase-separation mechanism and morphological control in all-polymer solar cells. *Acta Polym Sin*. 2018;2:145-163.
22. Zhang Y, Xu Y, Ford MJ, et al. Thermally stable all-polymer solar cells with high tolerance on blend ratios. *Adv Energy Mater*. 2018;8(18):1800029.
23. Meng Y, Wu J, Guo X, et al. 11.2% efficiency all-polymer solar cells with high open-circuit voltage. *Sci China Chem*. 2019;62(7):845-850.
24. Cheng P, Yan C, Li Y, Ma W, Zhan X. Diluting concentrated solution: a general, simple and effective approach to enhance efficiency of polymer solar cells. *Energ Environ Sci*. 2015;8(8):2357-2364.
25. Zhou Y, Kurosawa T, Ma W, et al. High performance all-polymer solar cell via polymer side-chain engineering. *Adv Mater*. 2014;26(22):3767-3772.
26. Wang L, Park JS, Lee HG, et al. Impact of chlorination patterns of naphthalenediimide-based polymers on aggregated structure, crystallinity, and device performance of all-polymer solar cells and organic transistors. *ACS Appl Mater Interfaces*. 2020;12(50):56240-56250.
27. Zhang ZG, Li Y. Polymerized small molecule acceptors for high performance all-polymer solar cells. *Angew Chem Int Ed*. 2020;60(9):4422-4433.
28. Sun H, Guo X, Facchetti A. High-performance n-type polymer semiconductors: applications, recent development, and challenges. *Chem*. 2020;6(6):1310-1326.

29. Yang J, Xiao B, Tang A, Li J, Wang X, Zhou E. Aromatic-diimide-based n-type conjugated polymers for all-polymer solar cell applications. *Adv Mater*. 2019;31(45):1804699.
30. Guo Y, Li Y, Awartani O, et al. Improved performance of all-polymer solar cells enabled by naphthodiperylenetetraimide-based polymer acceptor. *Adv Mater*. 2017;29(26):1700309.
31. Shi S, Chen P, Chen Y, et al. A narrow-bandgap n-type polymer semiconductor enabling efficient all-polymer solar cells. *Adv Mater*. 2019;31(46):1905161.
32. Feng K, Huang J, Zhang X, et al. High-performance all-polymer solar cells enabled by n-type polymers with an ultranarrow bandgap down to 1.28 eV. *Adv Mater*. 2020; 32(30):2001476.
33. Steyrleuthner R, Schubert M, Howard I, et al. Aggregation in a high-mobility n-type low-bandgap copolymer with implications on semicrystalline morphology. *J Am Chem Soc*. 2012; 134(44):18303-18317.
34. Mori D, Benten H, Okada I, Ohkita H, Ito S. Low-bandgap donor/acceptor polymer blend solar cells with efficiency exceeding 4%. *Adv Energy Mater*. 2014;4(3):1301006.
35. Kang H, Kim K-H, Choi J, Lee C, Kim BJ. High-performance all-polymer solar cells based on face-on stacked polymer blends with low interfacial tension. *ACS Macro Lett*. 2014; 3(10):1009-1014.
36. Mu C, Liu P, Ma W, et al. High-efficiency all-polymer solar cells based on a pair of crystalline low-bandgap polymers. *Adv Mater*. 2014;26(42):7224-7230.
37. Mori D, Benten H, Okada I, Ohkita H, Ito S. Highly efficient charge-carrier generation and collection in polymer/polymer blend solar cells with a power conversion efficiency of 5.7%. *Energ Environ Sci*. 2014;7(9):2939-2943.
38. Kang H, Uddin MA, Lee C, et al. Determining the role of polymer molecular weight for high-performance all-polymer solar cells: its effect on polymer aggregation and phase separation. *J Am Chem Soc*. 2015;137(6):2359-2365.
39. Gao L, Zhang Z-G, Xue L, et al. All-polymer solar cells based on absorption-complementary polymer donor and acceptor with high power conversion efficiency of 8.27%. *Adv Mater*. 2016;28(9):1884-1890.
40. Fan B, Ying L, Zhu P, et al. All-polymer solar cells based on a conjugated polymer containing siloxane-functionalized side chains with efficiency over 10%. *Adv Mater*. 2017;29(47): 1703906.
41. Li Z, Xie R, Zhong W, et al. High-performance green solvent processed ternary blended all-polymer solar cells enabled by complementary absorption and improved morphology. *Solar RRL*. 2018;2(10):1800196.
42. Li Z, Ying L, Xie R, et al. Designing ternary blend all-polymer solar cells with an efficiency of over 10% and a fill factor of 78%. *Nano Energy*. 2018;51:434-441.
43. Li Z, Ying L, Zhu P, et al. A generic green solvent concept boosting the power conversion efficiency of all-polymer solar cells to 11%. *Energ Environ Sci*. 2019;12(1):157-163.
44. Li Z, Zhong W, Ying L, et al. Morphology optimization via molecular weight tuning of donor polymer enables all-polymer solar cells with simultaneously improved performance and stability. *Nano Energy*. 2019;64:103931.
45. Zhang Q, Chen Z, Ma W, et al. Efficient nonhalogenated solvent-processed ternary all-polymer solar cells with a favorable morphology enabled by two well-compatible donors. *ACS Appl Mater Interfaces*. 2019;11(35):32200-32208.
46. Zhu L, Zhong W, Qiu C, et al. Aggregation-induced multi-length scaled morphology enabling 11.76% efficiency in all-polymer solar cells using printing fabrication. *Adv Mater*. 2019;31(41):1902899.
47. Park JS, Choi N, Lee C, et al. Elucidating roles of polymer donor aggregation in all-polymer and non-fullerene small-molecule–polymer solar cells. *Chem Mater*. 2020;32(8):3585-3596.
48. Chen D, Liu S, Liu J, Han J, Chen L, Chen Y. Regulation of the miscibility of the active layer by random terpolymer acceptors to realize high-performance all-polymer solar cells. *ACS Appl Polym Mater*. 2021;3(4):1923-1931.
49. Zhou N, Dudnik AS, Li TING, et al. All-polymer solar cell performance optimized via systematic molecular weight tuning of both donor and acceptor polymers. *J Am Chem Soc*. 2016; 138(4):1240-1251.
50. Schubert M, Dolfen D, Frisch J, et al. Influence of aggregation on the performance of all-polymer solar cells containing low-bandgap naphthalenediimide copolymers. *Adv Energy Mater*. 2012;2(3):369-380.
51. Roland S, Schubert M, Collins BA, et al. Fullerene-free polymer solar cells with highly reduced bimolecular recombination and field-independent charge carrier generation. *J Phys Chem Lett*. 2014;5(16):2815-2822.
52. Pavlopoulou E, Kim CS, Lee SS, et al. Tuning the morphology of all-polymer OPVs through altering polymer–solvent interactions. *Chem Mater*. 2014;26(17):5020-5027.
53. Zhang R, Yang H, Zhou K, et al. Molecular orientation and phase separation by controlling chain segment and molecule movement in P3HT/N2200 blends. *Macromolecules*. 2016; 49(18):6987-6996.
54. Zhou K, Wu Y, Liu Y, Zhou X, Zhang L, Ma W. Molecular orientation of polymer acceptor dominates open-circuit voltage losses in all-polymer solar cells. *ACS Energy Lett*. 2019;4(5): 1057-1064.
55. Chen S, Jung S, Cho HJ, et al. Highly flexible and efficient all-polymer solar cells with high-viscosity processing polymer additive toward potential of stretchable devices. *Angew Chem Int Ed*. 2018;57(40):13277-13282.
56. Balar N, Rech JJ, Henry R, et al. The importance of entanglements in optimizing the mechanical and electrical performance of all-polymer solar cells. *Chem Mater*. 2019;31(14): 5124-5132.
57. Lee C, Li Y, Lee W, et al. Correlation between phase-separated domain sizes of active layer and photovoltaic performances in all-polymer solar cells. *Macromolecules*. 2016; 49(14):5051-5058.
58. Ye L, Jiao X, Zhou M, et al. Manipulating aggregation and molecular orientation in all-polymer photovoltaic cells. *Adv Mater*. 2015;27(39):6046-6054.
59. Lee C, Giridhar T, Choi J, et al. Importance of 2d conjugated side chains of benzodithiophene-based polymers in controlling polymer packing, interfacial ordering, and composition variations of all-polymer solar cells. *Chem Mater*. 2017;29(21): 9407-9415.
60. Ye L, Zhang S, Huo L, Zhang M, Hou J. Molecular design toward highly efficient photovoltaic polymers based on two-

dimensional conjugated benzodithiophene. *Acc Chem Res*. 2014;47(5):1595-1603.
61. Deshmukh KD, Prasad SKK, Chandrasekaran N, et al. Critical role of pendant group substitution on the performance of efficient all-polymer solar cells. *Chem Mater*. 2017;29(2):804-816.
62. Kim HI, Kim M, Park CW, Kim HU, Lee H-K, Park T. Morphological control of donor/acceptor interfaces in all-polymer solar cells using a pentafluorobenzene-based additive. *Chem Mater*. 2017;29(16):6793-6798.
63. Zhou K, Zhang R, Liu J, et al. Donor/acceptor molecular orientation-dependent photovoltaic performance in all-polymer solar cells. *ACS Appl Mater Interfaces*. 2015;7(45):25352-25361.
64. Ye L, Jiao X, Zhao W, et al. Manipulation of domain purity and orientational ordering in high performance all-polymer solar cells. *Chem Mater*. 2016;28(17):6178-6185.
65. Robitaille A, Jenekhe SA, Leclerc M. Poly(naphthalene diimide-alt-bithiophene) prepared by direct (hetero)arylation polymerization for efficient all-polymer solar cells. *Chem Mater*. 2018;30(15):5353-5361.
66. Liu J, Zeng S, Zhang Z, Peng J, Liang Q. Optimizing the phase-separated domain size of the active layer via sequential crystallization in all-polymer solar cells. *J Phys Chem Lett*. 2020;11(6):2314-2321.
67. Lee J-W, Ma BS, Choi J, et al. Origin of the high donor–acceptor composition tolerance in device performance and mechanical robustness of all-polymer solar cells. *Chem Mater*. 2020;32(1):582-594.
68. Wang R, Yao Y, Zhang C, et al. Ultrafast hole transfer mediated by polaron pairs in all-polymer photovoltaic blends. *Nat Commun*. 2019;10(1):398.
69. Zhu P, Fan B, Ying L, Huang F, Cao Y. Recent progress in all-polymer solar cells based on wide-bandgap p-type polymers. *Chem Asian J*. 2019;14(18):3109-3118.
70. Zhong W, Hu Q, Jiang Y, et al. In situ structure characterization in slot-die-printed all-polymer solar cells with efficiency over 9%. *Solar RRL*. 2019;3(7):1900032.
71. Li K, Xie R, Zhong W, et al. 8.0% efficient all-polymer solar cells based on novel starburst polymer acceptors. *Sci China Chem*. 2018;61(5):576-583.
72. Xie B, Zhang K, Hu Z, et al. Polymer pre-aggregation enables optimal morphology and high performance in all-polymer solar cells. *Solar RRL*. 2020;4(3):1900385.
73. Earmme T, Hwang Y-J, Murari NM, Subramaniyan S, Jenekhe SA. All-polymer solar cells with 3.3% efficiency based on naphthalene diimide-selenophene copolymer acceptor. *J Am Chem Soc*. 2013;135(40):14960-14963.
74. Zhou N, Facchetti A. Naphthalenediimide (NDI) polymers for all-polymer photovoltaics. *Mater Today*. 2018;21(4):377-390.
75. Choi J, Kim K-H, Yu H, et al. Importance of electron transport ability in naphthalene diimide-based polymer acceptors for high-performance, additive-free, all-polymer solar cells. *Chem Mater*. 2015;27(15):5230-5237.
76. Earmme T, Hwang Y-J, Subramaniyan S, Jenekhe SA. All-polymer bulk heterojuction solar cells with 4.8% efficiency achieved by solution processing from a co-solvent. *Adv Mater*. 2014;26(35):6080-6085.
77. Hwang Y-J, Courtright BAE, Ferreira AS, Tolbert SH, Jenekhe SA. 7.7% efficient all-polymer solar cells. *Adv Mater*. 2015;27(31):4578-4584.
78. Oh J, Kranthiraja K, Lee C, et al. Side-chain fluorination: an effective approach to achieving high-performance all-polymer solar cells with efficiency exceeding 7%. *Adv Mater*. 2016;28(45):10016-10023.
79. Kim SW, Wang Y, You H, Lee W, Michinobu T, Kim BJ. Impact of incorporating nitrogen atoms in naphthalenediimide-based polymer acceptors on the charge generation, device performance, and stability of all-polymer solar cells. *ACS Appl Mater Interfaces*. 2019;11(39):35896-35903.
80. Kim M, Kim HI, Ryu SU, et al. Improving the photovoltaic performance and mechanical stability of flexible all-polymer solar cells via tailoring intermolecular interactions. *Chem Mater*. 2019;31(14):5047-5055.
81. Jia T, Zhang J, Zhong W, et al. 14.4% efficiency all-polymer solar cell with broad absorption and low energy loss enabled by a novel polymer acceptor. *Nano Energy*. 2020;72:104718.
82. Lee J-W, Sung MJ, Kim D, et al. Naphthalene diimide-based terpolymers with controlled crystalline properties for producing high electron mobility and optimal blend morphology in all-polymer solar cells. *Chem Mater*. 2020;32(6):2572-2582.
83. Cho H-H, Kim S, Kim T, et al. Design of cyanovinylene-containing polymer acceptors with large dipole moment change for efficient charge generation in high-performance all-polymer solar cells. *Adv Energy Mater*. 2018;8(3):1701436.
84. Deshmukh KD, Matsidik R, Prasad SKK, et al. Tuning the molecular weight of the electron accepting polymer in all-polymer solar cells: impact on morphology and charge generation. *Adv Funct Mater*. 2018;28(18):1707185.
85. Lee W, Lee C, Yu H, et al. Side chain optimization of naphthalenediimide–bithiophene-based polymers to enhance the electron mobility and the performance in all-polymer solar cells. *Adv Funct Mater*. 2016;26(10):1543-1553.
86. Kurosawa T, Gu X, Gu KL, et al. Understanding the impact of oligomeric polystyrene side chain arrangement on the all-polymer solar cell performance. *Adv Energy Mater*. 2018;8(2):1701552.
87. Kranthiraja K, Kim S, Lee C, et al. The impact of sequential fluorination of π-conjugated polymers on charge generation in all-polymer solar cells. *Adv Funct Mater*. 2017;27(29):1701256.
88. Kim SW, Choi J, Bui TTT, et al. Rationally designed donor–acceptor random copolymers with optimized complementary light absorption for highly efficient all-polymer solar cells. *Adv Funct Mater*. 2017;27(38):1703070.
89. Jung J, Lee W, Lee C, Ahn H, Kim BJ. Controlling molecular orientation of naphthalenediimide-based polymer acceptors for high performance all-polymer solar cells. *Adv Energy Mater*. 2016;6(15):1600504.
90. Lee C, Kang H, Lee W, et al. High-performance all-polymer solar cells via side-chain engineering of the polymer acceptor: the importance of the polymer packing structure and the nanoscale blend morphology. *Adv Mater*. 2015;27(15):2466-2471.
91. Cho H-H, Han G, Younts R, et al. Impact of highly crystalline, isoindigo-based small-molecular additives for enhancing the performance of all-polymer solar cells. *J Mater Chem A*. 2017;5(40):21291-21299.
92. You H, Kim D, Cho H-H, et al. Shift of the branching point of the side-chain in naphthalenediimide (NDI)-based polymer

for enhanced electron mobility and all-polymer solar cell performance. *Adv Funct Mater*. 2018;28(39):1803613.

93. Li Z, Xu X, Zhang W, et al. High performance all-polymer solar cells by synergistic effects of fine-tuned crystallinity and solvent annealing. *J Am Chem Soc*. 2016;138(34):10935-10944.
94. Lin Y, Dong S, Li Z, et al. Energy-effectively printed all-polymer solar cells exceeding 8.61% efficiency. *Nano Energy*. 2018;46:428-435.
95. Liu X, Zhang C, Duan C, et al. Morphology optimization via side chain engineering enables all-polymer solar cells with excellent fill factor and stability. *J Am Chem Soc*. 2018; 140(28):8934-8943.
96. Diao Y, Zhou Y, Kurosawa T, et al. Flow-enhanced solution printing of all-polymer solar cells. *Nat Commun*. 2015;6(1): 7955.
97. Zhou E, Cong J, Hashimoto K, Tajima K. Control of miscibility and aggregation via the material design and coating process for high-performance polymer blend solar cells. *Adv Mater*. 2013;25(48):6991-6996.
98. Liu S, Chen D, Zhou W, et al. Vertical distribution to optimize active layer morphology for efficient all-polymer solar cells by j71 as a compatibilizer. *Macromolecules*. 2019;52(11):4359-4369.
99. Kim SW, Kim H, Lee J-W, et al. Synergistic effects of terpolymer regioregularity on the performance of all-polymer solar cells. *Macromolecules*. 2019;52(2):738-746.
100. Fan B, Zhong W, Ying L, et al. Surpassing the 10% efficiency milestone for 1-cm^2 all-polymer solar cells. *Nat Commun*. 2019;10(1):4100.
101. Zhao J, Li Y, Yang G, et al. Efficient organic solar cells processed from hydrocarbon solvents. *Nat Energy*. 2016;1: 15027.
102. Mori D, Benten H, Kosaka J, Ohkita H, Ito S, Miyake K. Polymer/polymer blend solar cells with 2.0% efficiency developed by thermal purification of nanoscale-phase-separated morphology. *ACS Appl Mater Interfaces*. 2011;3(8):2924-2927.
103. Mori D, Benten H, Ohkita H, Ito S, Miyake K. Polymer/polymer blend solar cells improved by using high-molecular-weight fluorene-based copolymer as electron acceptor. *ACS Appl Mater Interfaces*. 2012;4(7):3325-3329.
104. Zhou K, Liu J, Li M, Yu X, Xing R, Han Y. Phase diagram of conjugated polymer blend P3HT/PF12TBT and the morphology-dependent photovoltaic performance. *J Phys Chem C*. 2015;119(4):1729-1736.
105. Zhou K, Liu J, Zhang R, et al. The molecular regioregularity induced morphological evolution of polymer blend thin films. *Polymer*. 2016;86:105-112.
106. Zhou K, Liu J, Li M, Yu X, Xing R, Han Y. Decreased domain size and improved crystallinity by adjusting solvent–polymer interaction parameters in all-polymer solar cells. *J Polym Sci B*. 2015;53(4):288-296.
107. Yu W, Yang D, Zhu X, et al. Control of nanomorphology in all-polymer solar cells via assembling nanoaggregation in a mixed solution. *ACS Appl Mater Interfaces*. 2014;6(4):2350-2355.
108. Zhan X, Za T, Domercq B, et al. A high-mobility electron-transport polymer with broad absorption and its use in field-effect transistors and all-polymer solar cells. *J Am Chem Soc*. 2007;129(23):7246-7247.
109. Zhao X, Zhan X. Electron transporting semiconducting polymers in organic electronics. *Chem Soc Rev*. 2011;40(7):3728-3743.
110. Zhang Y, Wan Q, Guo X, et al. Synthesis and photovoltaic properties of an n-type two-dimension-conjugated polymer based on perylene diimide and benzodithiophene with thiophene conjugated side chains. *J Mater Chem A*. 2015;3(36): 18442-18449.
111. Hwang Y-J, Earmme T, Courtright BAE, Eberle FN, Jenekhe SA. N-type semiconducting naphthalene diimide-perylene diimide copolymers: controlling crystallinity, blend morphology, and compatibility toward high-performance all-polymer solar cells. *J Am Chem Soc*. 2015; 137(13):4424-4434.
112. Guo Y, Li Y, Awartani O, et al. A vinylene-bridged perylenediimide-based polymeric acceptor enabling efficient all-polymer solar cells processed under ambient conditions. *Adv Mater*. 2016;28(38):8483-8489.
113. Cheng P, Ye L, Zhao XG, Hou JH, Li YF, Zhan XW. Binary additives synergistically boost the efficiency of all-polymer solar cells up to 3.45%. *Energ Environ Sci*. 2014;7(4):1351-1356.
114. Ye L, Xiong Y, Li S, et al. Precise manipulation of multi-length scale morphology and its influence on eco-friendly printed all-polymer solar cells. *Adv Funct Mater*. 2017;27: 1702016.
115. Zhou Y, Gu KL, Gu XD, et al. All-polymer solar cells employing non-halogenated solvent and additive. *Chem Mater*. 2016;28(14):5037-5042.
116. Gu X, Zhou Y, Gu K, et al. Roll-to-roll printed large-area all-polymer solar cells with 5% efficiency based on a low crystallinity conjugated polymer blend. *Adv Energy Mater*. 2017; 7(14):1602742.
117. Ye L, Xiong Y, Yao H, et al. High performance organic solar cells processed by blade coating in air from a benign food additive solution. *Chem Mater*. 2016;28(20):7451-7458.
118. Li S, Zhang H, Zhao W, et al. Green-solvent-processed all-polymer solar cells containing a perylene diimide-based acceptor with an efficiency over 6.5%. *Adv Energy Mater*. 2016; 6(5):1501991.
119. Zhao R, Liu J, Wang L. Polymer acceptors containing B←N units for organic photovoltaics. *Acc Chem Res*. 2020;53(8): 1557-1567.
120. Li Y, Meng H, Liu T, et al. 8.78% efficient all-polymer solar cells enabled by polymer acceptors based on a B←N embedded electron-deficient unit. *Adv Mater*. 2019;31(44):1904585.
121. Dou C, Liu J, Wang L. Conjugated polymers containing B←N unit as electron acceptors for all-polymer solar cells. *Sci China Chem*. 2017;60(4):450-459.
122. Wang N, Long X, Ding Z, et al. Improving active layer morphology of all-polymer solar cells by dissolving the two polymers individually. *Macromolecules*. 2019;52(6):2402-2410.
123. Wang N, Yu Y, Zhao R, Ding Z, Liu J, Wang L. Improving active layer morphology of all-polymer solar cells by solution temperature. *Macromolecules*. 2020;53(9):3325-3331.

124. Zhang L, Ding Z, Zhao R, et al. Effect of polymer donor aggregation on the active layer morphology of amorphous polymer acceptor-based all-polymer solar cells. *J Mater Chem C*. 2020; 8(16):5613-5619.
125. Ding Z, Zhao R, Yu Y, Liu J. All-polymer indoor photovoltaics with high open-circuit voltage. *J Mater Chem A*. 2019;7(46): 26533-26539.
126. Zhao C, Guo Y, Zhang Y, Yan N, You S, Li W. Diketopyrrolopyrrole-based conjugated materials for non-fullerene organic solar cells. *J Mater Chem A*. 2019;7(17): 10174-10199.
127. Falzon MF, Zoombelt AP, Wienk MM, Janssen RA. Diketopyrrolopyrrole-based acceptor polymers for photovoltaic application. *Phys Chem Chem Phys*. 2011;13(19):8931-8939.
128. Li W, An Y, Wienk MM, Janssen RAJ. Polymer–polymer solar cells with a near-infrared spectral response. *J Mater Chem A*. 2015;3(13):6756-6760.
129. Li Z, Xu X, Zhang W, et al. High-photovoltage all-polymer solar cells based on a diketopyrrolopyrrole–isoindigo acceptor polymer. *J Mater Chem A*. 2017;5(23):11693-11700.
130. Zhang A, Xiao C, Meng D, et al. Conjugated polymers with deep LUMO levels for field-effect transistors and polymer–polymer solar cells. *J Mater Chem C*. 2015;3(31):8255-8261.
131. Li W, Roelofs WS, Turbiez M, Wienk MM, Janssen RA. Polymer solar cells with diketopyrrolopyrrole conjugated polymers as the electron donor and electron acceptor. *Adv Mater*. 2014; 26(20):3304-3309.
132. Yu Y, Zhou S, Wang X, et al. Enhancing the performance of non-fullerene solar cells with polymer acceptors containing large-sized aromatic units. *Org Electron*. 2017;47:133-138.
133. Long X, Ding Z, Dou C, Zhang J, Liu J, Wang L. Polymer acceptor based on double B←N bridged bipyridine (BNBP) unit for high-efficiency all-polymer solar cells. *Adv Mater*. 2016;28(30):6504-6508.
134. Jiang Z, Ni Z, Wang H, et al. Versatile asymmetric thiophene/benzothiophene flanked diketopyrrolopyrrole polymers with ambipolar properties for OFETs and OSCs. *Polym Chem*. 2017;8(36):5603-5610.
135. Long X, Wang N, Ding Z, Dou C, Liu J, Wang L. Low-bandgap polymer electron acceptors based on double B ← N bridged bipyridine (BNBP) and diketopyrrolopyrrole (DPP) units for all-polymer solar cells. *J Mater Chem C*. 2016;4(42): 9961-9967.
136. Zhang A, Wang Q, Bovee RAA, et al. Perfluoroalkyl-substituted conjugated polymers as electron acceptors for all-polymer solar cells: the effect of diiodoperfluoroalkane additives. *J Mater Chem A*. 2016;4(20):7736-7745.
137. Chen H-Y, Nikolka M, Wadsworth A, et al. A thieno[2,3-b] pyridine-flanked diketopyrrolopyrrole polymer as an n-type polymer semiconductor for all-polymer solar cells and organic field-effect transistors. *Macromolecules*. 2017;51(1):71-79.
138. Li Y, Jia Z, Zhang Q, et al. Toward efficient all-polymer solar cells via halogenation on polymer acceptors. *ACS Appl Mater Interfaces*. 2020;12(29):33028-33038.
139. Wang W, Wu Q, Sun R, et al. Controlling molecular mass of low-band-gap polymer acceptors for high-performance all-polymer solar cells. *Joule*. 2020;4(5):1070-1086.
140. Fan Q, Xiao Z, Wang E, Ding L. Polymer acceptors based on Y6 derivatives for all-polymer solar cells. *Sci Bul*. 2021;66(19): 1950-1953.
141. Yao H, Bai F, Hu H, et al. Efficient all-polymer solar cells based on a new polymer acceptor achieving 10.3% power conversion efficiency. *ACS Energy Lett*. 2019;4(2): 417-422.
142. Wu J, Meng Y, Guo X, Zhu L, Liu F, Zhang M. All-polymer solar cells based on a novel narrow-bandgap polymer acceptor with power conversion efficiency over 10%. *J Mater Chem A*. 2019;7(27):16190-16196.
143. Du J, Hu K, Meng L, et al. High-performance all-polymer solar cells: synthesis of polymer acceptor by a random ternary copolymerization strategy. *Angew Chem Int Ed*. 2020;59(35): 15181-15185.
144. Yu H, Pan M, Sun R, et al. Regio-regular polymer acceptors enabled by determined fluorination on end groups for all-polymer solar cells with 15.2% efficiency. *Angew Chem Int Ed*. 2021;60(18):10137-10146.
145. Luo Z, Liu T, Ma R, et al. Precisely controlling the position of bromine on the end group enables well-regular polymer acceptors for all-polymer solar cells with efficiencies over 15%. *Adv Mater*. 2020;32(48):2005942.
146. Fu H, Li Y, Yu J, et al. High efficiency (15.8%) all-polymer solar cells enabled by a regioregular narrow bandgap polymer acceptor. *J Am Chem Soc*. 2021;143(7):2665-2670.
147. Moore JR, Albert-Seifried S, Rao A, et al. Polymer blend solar cells based on a high-mobility naphthalenediimide-based polymer acceptor: device physics, photophysics and morphology. *Adv Energy Mater*. 2011;1(2):230-240.
148. Feng S, Liu C, Xu X, et al. Siloxane-terminated side chain engineering of acceptor polymers leading to over 7% power conversion efficiencies in all-polymer solar cells. *ACS Macro Lett*. 2017;6(11):1310-1314.
149. Li Z, Fan B, He B, et al. Side-chain modification of polyethylene glycol on conjugated polymers for ternary blend all-polymer solar cells with efficiency up to 9.27%. *Sci China Chem*. 2018;61(4):427-436.
150. Xu X, Feng K, Yu L, Yan H, Li R, Peng Q. Highly efficient all-polymer solar cells enabled by p-doping of the polymer donor. *ACS Energy Lett*. 2020;5(7):2434-2443.
151. Gao M, Wang W, Hou J, Ye L. Control of aggregated structure of photovoltaic polymers for high-efficiency solar cells. *Aggregate*. 2021;2(5):e46.
152. Jiang X, Yang J, Karuthedath S, et al. Miscibility-controlled phase separation in double-cable conjugated polymers for single-component organic solar cells with efficiencies over 8%. *Angew Chem Int Ed*. 2020;59(48):21683-21692.
153. Liu F, Li C, Li J, et al. Ternary organic solar cells based on polymer donor, polymer acceptor and PCBM components. *Chin Chem Lett*. 2020;31(3):865-868.
154. Yan N, Zhao C, You S, Zhang Y, Li W. Recent progress of thin-film photovoltaics for indoor application. *Chin Chem Lett*. 2020;31(3):643-653.
155. Liu Y, Xian K, Peng Z, et al. Tuning the molar mass of P3HT via direct arylation polycondensation yields optimal interaction and high efficiency in nonfullerene organic solar cells. *J Mater Chem A*. 2021;9(35):19874-19885.
156. Savikhin V, Shapiro DA, Gu X, Oosterhout SD, Toney MF. Ptychography of organic thin films at soft x-ray energies. *Chem Mater*. 2019;31(13):4913-4918.
157. Ye L, Stuard S, Ade H. Soft x-ray scattering characterization of polymer semiconductors. In: Reynolds JR, Thompson BC,

Skotheim TA, eds. *Conjugated Polymers: Properties, Processing, and Applications*. CRC Press; 2019 Chap 13.

158. Liu F, Brady MA, Wang C. Resonant soft X-ray scattering for polymer materials. *Eur Polym J*. 2016;81:555-568.
159. Swaraj S, Wang C, Yan H, et al. Nanomorphology of bulk heterojunction photovoltaic thin films probed with resonant soft X-ray scattering. *Nano Lett*. 2010;10(8):2863-2869.
160. Yan H, Collins BA, Gann E, Wang C, Ade H, McNeill CR. Correlating the efficiency and nanomorphology of polymer blend solar cells utilizing resonant soft X-ray scattering. *ACS Nano*. 2012;6(1):677-688.
161. Collins BA, Cochran JE, Yan H, et al. Polarized X-ray scattering reveals non-crystalline orientational ordering in organic films. *Nat Mater*. 2012;11(6):536-543.
162. Litofsky JH, Lee Y, Aplan MP, et al. Polarized soft X-ray scattering reveals chain orientation within nanoscale polymer domains. *Macromolecules*. 2019;52(7):2803-2813.
163. Ye L, Jiao XC, Zhang H, et al. 2D-conjugated benzodithiophene-based polymer acceptor: design, synthesis, nanomorphology, and photovoltaic performance. *Macromolecules*. 2015;48(19):7156-7163.
164. Wirix MJM, Bomans PHH, Hendrix MMRM, Friedrich H, Sommerdijk NAJM, de With G. Visualizing order in dispersions and solid state morphology with Cryo-TEM and electron tomography: P3HT : PCBM organic solar cells. *J Mater Chem A*. 2015;3(9):5031-5040.
165. Yao Z-F, Wang Z-Y, Wu H-T, et al. Ordered solid-state microstructures of conjugated polymers arising from solution-state aggregation. *Angew Chem Int Ed*. 2020;59(40):17467-17471.
166. Liu J, Gao M, Kim J, et al. Challenges and recent advances in photodiodes-based organic photodetectors. *Mater Today*. 2021;51:475-503.
167. Ye L, Collins B, Jiao X, Zhao J, Yan H, Ade H. Miscibility-function relations in organic solar cells: significance of optimal miscibility in relation to percolation. *Adv Energy Mater*. 2018;8(28):1703058.
168. Treat ND, Varotto A, Takacs CJ, et al. Polymer-fullerene miscibility: a metric for screening new materials for high-performance organic solar cells. *J Am Chem Soc*. 2012;134(38):15869-15879.
169. Gao M, Liang Z, Geng Y, Ye L. Significance of thermodynamic interaction parameters in guiding the optimization of polymer:nonfullerene solar cells. *Chem Commun*. 2020;56(83):12463-12478.
170. Peng Z, Xian K, Cui Y, et al. Thermoplastic elastomer tunes phase structure and promotes stretchability of high-efficiency organic solar cells. *Adv Mater*. 2021;33(49):2106732.
171. Peng Z, Jiang K, Qin Y, et al. Modulation of morphological, mechanical, and photovoltaic properties of ternary organic photovoltaic blends for optimum operation. *Adv Energy Mater*. 2021;11(8):2003506.

AUTHOR BIOGRAPHIES

Kangkang Zhou earned his Bachelor's and Master's degree in Polymer Materials and Engineering from Zhengzhou University in July 2020. Presently, He is a Ph.D. student at the School of Materials Science and Engineering, Tianjin University under the supervision of Prof. Long Ye and Prof. Yanhou Geng. His research work focuses on understanding the relations between morphology and mechanical properties of conjugated polymer blends used in high-efficiency solar cells.

Kaihu Xian is currently a Ph.D. candidate at the School of Materials Science and Engineering of Tianjin University since October 2020 under the supervision of Prof. Long Ye and Prof. Yanhou Geng. He received his Master's degree from the Institute of Chemistry, Chinese Academy of Sciences (ICCAS) in 2020. His current research focuses on the device engineering and materials physics of low-cost organic/polymer conjugated materials in solar cells.

Long Ye has been a Professor at the School of Materials Science and Engineering of Tianjin University since October 2019. He received his Ph.D. degree from ICCAS in 2015 (Adviser: Prof. Jianhui Hou). From 2015 to 2019, he was a postdoctoral researcher and later promoted to research assistant professor in the same group headed by Prof. Harald Ade at the Department of Physics, North Carolina State University. His current interests include morphological and mechanical characterizations of semiconducting polymers and their blends in solar cells and transistors, and polymer physics of conjugated polymers.

How to cite this article: Zhou K, Xian K, Ye L. Morphology control in high-efficiency all-polymer solar cells. *InfoMat*. 2022;4(4):e12270. doi:10.1002/inf2.12270